



**Ministry of Environment
and Gender Equality**

Environmental
Protection Agency

Development of an SCR system integrating a novel reductant delivery system

MUDP Report

May 2025

Publisher: The Danish Environmental Protection Agency

Editors:

Jim Elkjær Bebe, Dinex A/S

Fabian Feldhaus, Albonair GmbH

Ivar Lund, Syddansk Universitet

ISBN: 978-87-7564-002-7

Miljøstyrelsen offentliggør rapporter og indlæg vedrørende forsknings- og udviklingsprojekter inden for miljøsektoren, som er finansieret af Miljøstyrelsen. Det skal bemærkes, at en sådan offentliggørelse ikke nødvendigvis betyder, at det pågældende indlæg giver udtryk for Miljøstyrelsens synspunkter. Offentliggørelsen betyder imidlertid, at Miljøstyrelsen finder, at indholdet udgør et væsentligt indlæg i debatten omkring den danske miljøpolitik.

Må citeres med kildeangivelse.

Contents

1.	Experimentation	5
1.1	Experimental Setup	5
1.2	Droplet Statistics	5
1.2.1	Mean Diameters	5
1.3	Comparison of PDA and Shadow Sizing Measurement Technology	6
1.4	Optimized Sampling Grid for PDA Point Measurement	8
1.5	Repeatability of Droplet Measurements with Different Nozzle Orientations	8
1.6	Analysis of Spray Atomization	9
1.7	Summary	10
2.	Numerical Modelling of the Heated Nozzle	11
2.1	Determination of the Cone Angle	12
2.2	Determination of Initial Velocity	12
2.3	Validation and Results	13
2.4	Summary	14
3.	Development of Full Aftertreatment System	15
3.1	Adaptation and application of the heated nozzle CFD model	15
3.2	Heated nozzle simulation results and calibration (sub model)	16
3.3	Model Validation	18
3.3.1	NH ₃ Uniformity	18
3.3.2	Spray Propagation	18
3.4	Mixer Development	19
3.4.1	Performance	20
3.4.2	Durability	21
3.4.3	Manufacturability	23
3.5	Summary	24
4.	Software and Testing Support	25
4.1	Introduction and Working Principles of the Heated Nozzle	25
4.2	Components of the Dosing System and Their Functionality	26
4.3	Software and Controls	26
4.4	Support During Project Execution	27
5.	Optimization of Prototype	28
5.1	Optimizations Due to Market Demand	28
5.2	Geometrical (Design) Optimization	29
5.3	NH ₃ Conversion Optimization	29
5.4	Controls Improvement	30
6.	System Validation	32
6.1	Benchmark Testing and Comparison to the Conventional Nozzle	32
6.1.1	NH ₃ UI Testing	32
6.1.2	Transient Hot- and Cold Cycle Testing	33
6.1.3	Transient Testing – Reduced Temperature Release	35
6.2	Bespoke Mixer Testing	36

6.2.1	Prototyping and Installation	36
6.2.2	Backpressure Testing	37
6.2.3	Bespoke Mixer, NH3 UI Tests	38
6.2.4	Deposit Testing	39
6.3	Discussion	39
7.	Dissemination	41
7.1	19th FAD-Conference “Challenge – Exhaust Aftertreatment”	41
7.2	IAA 2022	41
7.3	ECT-2023 ECMA’s 14 th International Conference “Leaping to cleaner air for tomorrow”	42
7.4	AVL SIMpulse: Alternative Fuels for Internal Combustion Engines – Myth or Opportunity?	42
7.5	Status at the Closure of the Project	42
8.	References	43

1. Experimentation

Knowledge about the spray atomization characterisation for the SCR injection system is important for the understanding and the optimization of the heated nozzle system. The experimental data is also used for validation of the simulations described in Chapter 2.

1.1 Experimental Setup

The experimental setup consisted of two types of experiments conducted on the heated nozzle. A 2D Phase Doppler Anemometry (PDA) by Dantec Dynamics was used to record diameter statistics in the secondary atomization region of the spray. The primary atomization region (less than 10 mm) was recorded using back-light imaging. The experimental setup for the two types can be seen in FIGURE 1.

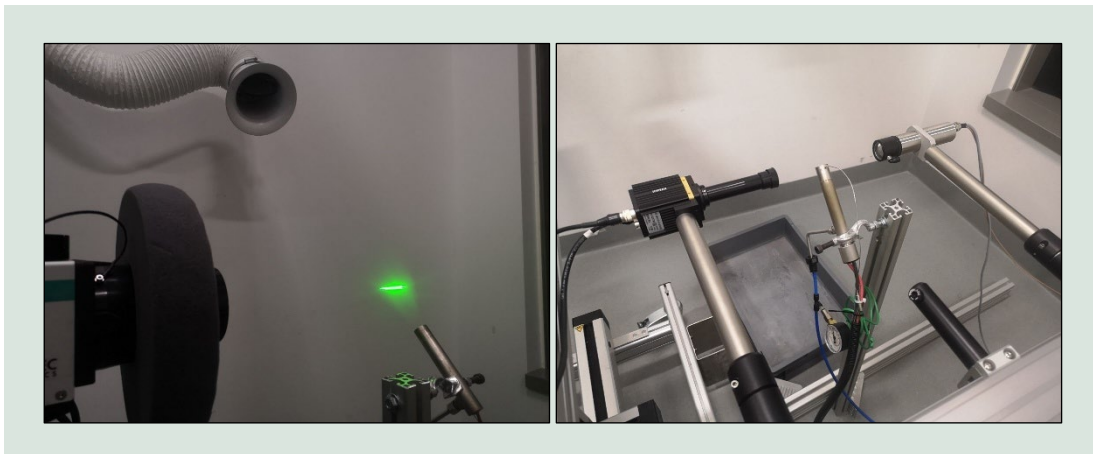


FIGURE 1. PDA setup for nozzle characterization (left) and back-light imaging setup (right)

1.2 Droplet Statistics

Different droplet statistics measures will be used to quantify the feasibility of the different nozzle prototypes as well as the influence of the different test parameters. The definitions are listed below.

1.2.1 Mean Diameters

Means diameters are only calculated with the BSA P processor. In the Diameter statistics, D_i is the diameter of the size class i , N_i the number of size classes (bins), n_i the number of particles in each size class and N the total number of particles.

D10

The **arithmetic mean diameter** is the ensemble or (arithmetic) number mean diameter of the acquired and validated samples:

$$D_{10} = \frac{1}{N} \sum_{i=1}^{N_i} n_i D_i$$

D20

The **area mean diameter** is calculated from the mean squared diameters:

$$D_{20} = \left\{ \frac{1}{N} \sum_{i=1}^{N_i} n_i D_i^2 \right\}^{\frac{1}{2}}$$

D30

The **volume mean diameter** is calculated from the mean of the droplet volumes:

$$D_{30} = \left\{ \frac{1}{N} \sum_{i=1}^{N_i} n_i D_i^3 \right\}^{\frac{1}{3}}$$

D32

The Sauter mean diameter (SMD) is calculated as:

$$D_{32} = \frac{\sum_{i=1}^{N_i} n_i D_i^3}{\sum_{i=1}^{N_i} n_i D_i^2}$$

Dv(xx)

The fractional volume diameters represent the particle diameters below which 10%, 50%, 90% of the total volume is contained, i.e. where the cumulative function of the volume distribution (xx) has the value 0.1, 0.5 or 0.9 respectively.

Span

The span is an indicator for the width of a size distribution. This parameter describes the steepness of the cumulative curve of the volume distribution:

$$Span = \frac{D_{V0.9} - D_{V0.1}}{D_{V0.5}} \cdot 100\%$$

1.3 Comparison of PDA and Shadow Sizing Measurement Technology

The first version of the heated nozzle was analyzed in the spray lab at SDU. The test was conducted with water at a mass flow rate of 700 g/h and a nozzle temperature of 230°C. The water was sprayed into quiescent surroundings with an air temperature of approximately 20°C. Droplet data was collected in a plane normal to the spray at distance 55 mm away from the nozzle.

The images obtained from back-light imaging can be seen from FIGURE 2 which were then processed in specifically developed python routines and the data obtained from both the measurement systems was then compared. This comparison at a distance of 55 mm away from the nozzle was plotted in terms of Probability Density Function of droplet diameters and can be seen in FIGURE 3 **Fejl! Henvisningskilde ikke fundet.** The obtained results clearly indicated very similar droplet diameter distributions obtained from the two measurement systems. Therefore, PDA was adopted as the main measurement equipment as the data obtained from PDA was easy to post-process as compared with processing of images obtained from the back-light imaging.

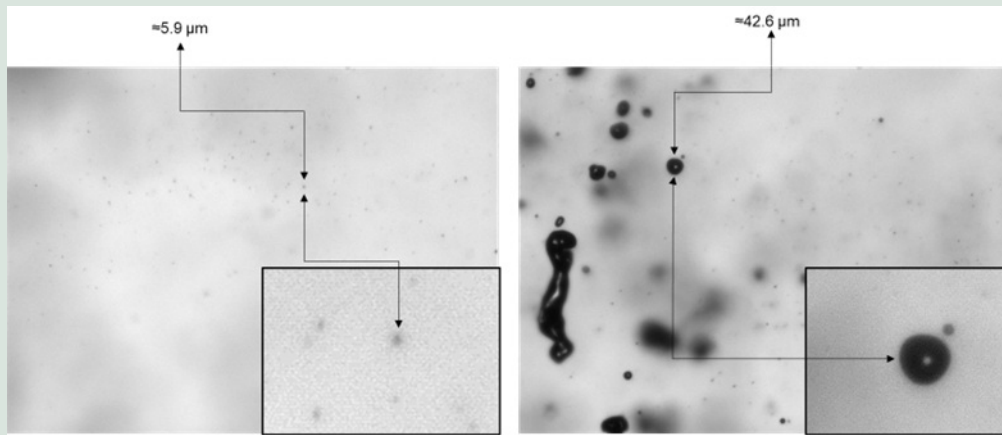


FIGURE 2. Images obtained from back-light imaging (test fluid was water)

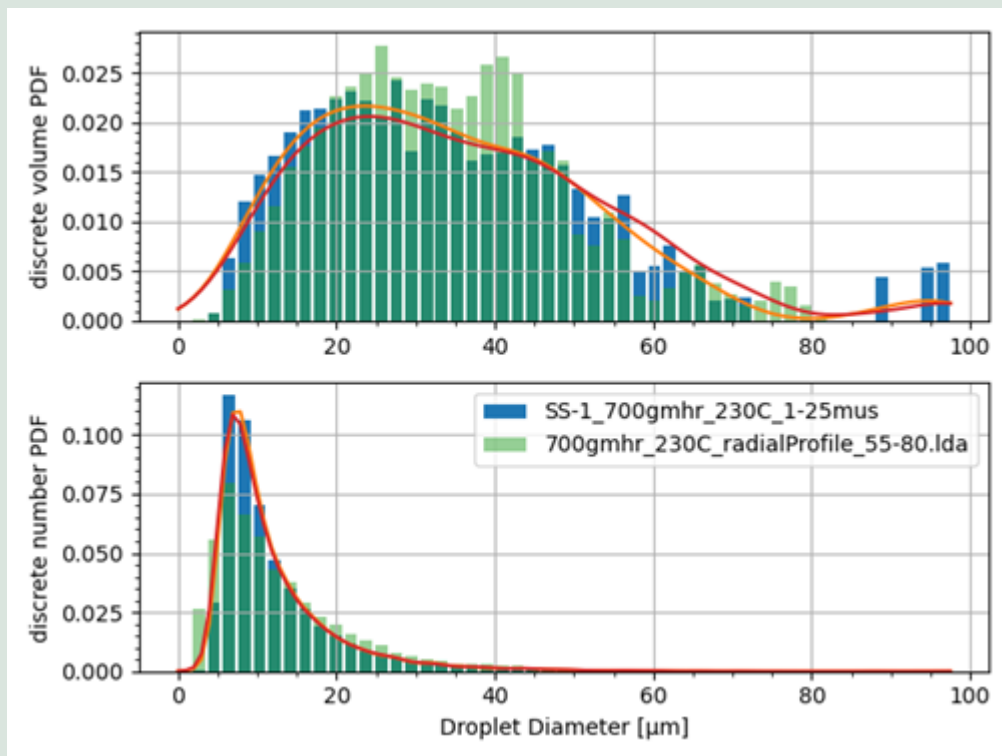


FIGURE 3. Comparison of data obtained from PDA (green) and back-light imaging (blue) at a distance of 55 mm from the nozzle tip (test fluid was water). Dark green indicates an overlap between the two.

The droplet statistics for the radial measurement at 55 mm away from the nozzle tip can be seen in TABLE 1Fejl! Henvisningskilde ikke fundet.. The mass flow rate was 700 g/h and the test fluid was water.

TABLE 1. Droplet statistics with a flowrate of 700 g/h in a measurement plane 55 mm from the nozzle tip.

Mass flow rate	Nozzle set-point temperature	Distance to measurement plane	Mean axial velocity	Mean diameter				Fractional volume diameter			
				D10	D20	D30	D32	Dv0.1	Dv0.5	Dv0.9	Span
[g/h]	[°C]	[mm]	[m/s]	[μm]	[μm]	[μm]	[μm]				
700	20	55	13,0	13,0	15,9	18,9	26,9	15,9	33,1	54,3	1,16

1.4 Optimized Sampling Grid for PDA Point Measurement

Several iterations in developing an optimized sampling grid for point measurement of droplet data were investigated and the final grid is illustrated in **Fejl! Henvisningskilde ikke fundet.** The grid was designed to capture every single droplet in a plane normal to the flow direction and at a specific distance.

The standard grid was 10, 30 and 100 mm from the nozzle tip. Each plane contained 50 measurement points. The orientation of the nozzle in the test setup was mainly 45° upwards (see **FIGURE 1Fejl! Henvisningskilde ikke fundet.**).

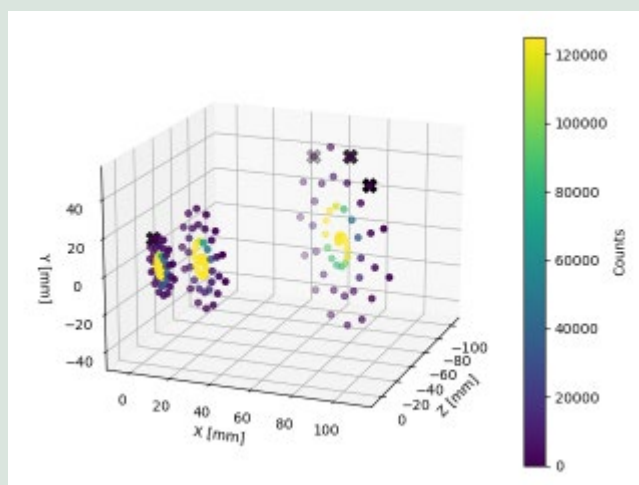


FIGURE 4. Count rate obtained in the measurement mesh

FIGURE 4Fejl! Henvisningskilde ikke fundet. shows the counts (number of droplets recorded) at the single measurement points in a particular magnitude of time. Generally, a high-count rate was observed in the central axis with the nozzle tip which was seen to decrease in the outer region of the cone. 'X' in **FIGURE 4Fejl! Henvisningskilde ikke fundet.** shows the measurement points where no droplets were recorded by the PDA measurement. This was an indication that the measurement mesh grid was covering the whole of the spray cone produced by the nozzle.

1.5 Repeatability of Droplet Measurements with Different Nozzle Orientations

The effect of different nozzle orientation was investigated for 45° upwards and 45° downwards and the repeatability of the test methodology was analyzed by conducting a repeated test. Illustration of the nozzle angle can be seen in **FIGURE 5.**

The test was conducted in the 3 different measurement planes, as illustrated in **FIGURE 4.** The effect of change in injection angle and the repeatability of the measurements using urea-

water solution can be seen in Figure 6. A change of injection angle from +45 to -45 had little or no effect on the droplet distribution produced by the nozzle. Therefore, the nozzle can be mounted in any orientation in the actual SCR system without producing any compromise on the droplet diameter distribution produced. The repeatability check indicated that the measurement droplet distributions were highly repeatable with little or no variation over a period.

1	45° bottom-up	
2	45° top-down	
3	90° top-down.	

FIGURE 5. Orientation of the nozzle.

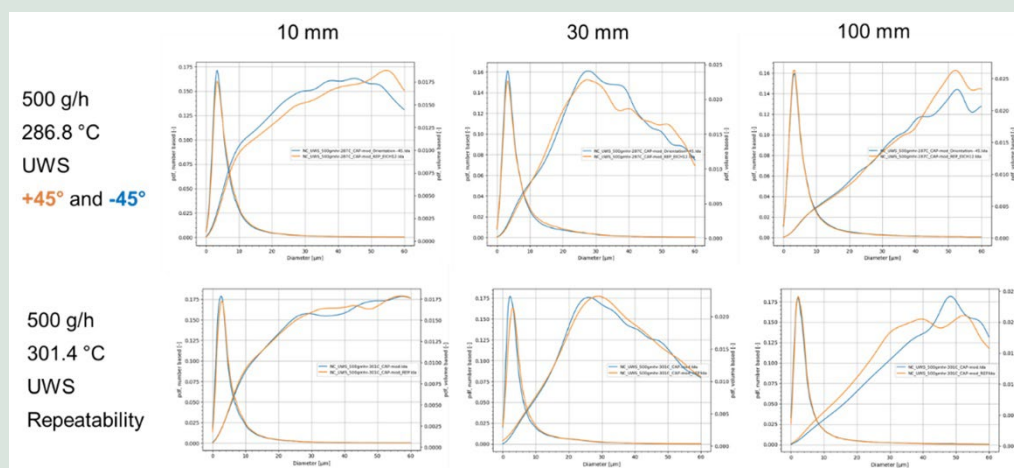


FIGURE 6. Check on the orientation of the nozzle and the repeatability of the measurements.

1.6 Analysis of Spray Atomization

PDA measurements were conducted in the urea spray generated with the heated nozzle (EICH14 with modified cap) in a 45° bottom-up orientation. The urea-water solution was sprayed into quiescent surroundings with air temperature of approximately 20°C. Data was collected in FIGURE 3 separate planes normal to the spray direction and with 10, 30 and 100 mm distance from the nozzle.

The different test conditions as well as droplet statistics can be seen in TABLE 2. The spherical validation was expected to increase downstream the nozzle exit, because the region close to the nozzle tip normally has a lot of non-spherical droplets and PDA methodology is a technique which applies only to spherical droplet. However, this was not the case for the range of 10 to 100 mm (TABLE 2). On the other hand, the spherical validation was increased with higher flowrates, e.g., approx. 50% validation rate for a flowrate of 50 g/h and approx. 80% for a flowrate of 1000 g/h.

In general, the mean droplet velocity decreased from the 10 mm distance plane to the 100 mm distance plane. Looking at the droplet sizes, the mean droplet size also decreased for the

mass flow rate 1000 and 1500 g/h. It was not the case for lower mass flow rates. Another finding was that increasing the mass flow rate also affected a higher droplet velocity and mean droplet size and a larger span.

TABLE 2. Droplet statistics at different flowrates and measurement grids (liquid medium: UWS, +45° nozzle orientation, Nozzle EICH14 with modified cap).

Mass flow rate	Nozzle setpoint temperature	Distance to measurement plane	Mean axial velocity	Mean diameter				Fractional volume diameter			
				D10	D20	D30	D32	Dv0.1	Dv0.5	Dv0.9	Span
[g/h]	[°C]	[mm]	[m/s]	[µm]	[µm]	[µm]	[µm]	[µm]	[µm]	[µm]	[µm]
50	196,2	10	2,1	2,1	3,8	8,2	37,2	38,6	64,6	71,1	0,503
		30	1,4	2,9	5,9	11,6	44,9	40,0	65,3	71,1	0,475
		100	0,8	2,7	3,7	6,3	22,1	6,9	66,0	71,1	0,973
100	211,4	10	3,0	2,0	3,0	6,0	25,3	27,8	64,6	71,1	0,670
		30	2,0	2,5	4,4	9,0	37,9	37,9	64,6	70,3	0,503
		100	0,9	2,5	3,2	5,1	13,0	4,0	63,1	71,8	1,060
350	273,8	10	9,0	7,7	12,4	17,4	34,8	20,6	48,0	67,5	0,977
		30	5,1	7,7	12,9	17,9	34,5	22,0	42,9	64,6	0,992
		100	2,5	7,8	13,6	19,6	40,4	26,3	50,9	68,2	0,823
500	301,4	10	9,0	8,5	12,7	17,2	31,9	18,4	42,9	65,3	1,090
		30	5,8	8,2	12,6	16,9	30,6	19,8	37,2	62,4	1,150
		100	3,0	6,3	10,5	15,2	32,2	19,8	42,9	63,1	1,010
1000	354,2	10	13,4	7,5	11,6	16,1	31,2	18,4	42,2	64,6	1,090
		30	7,9	5,8	9,9	14,4	30,7	19,8	38,6	61,4	1,100
		100	3,8	3,7	6,0	9,8	25,8	14,1	42,9	64,6	1,180
1500	372,7	10	19,1	7,4	10,5	14,5	27,8	14,8	40,8	64,6	1,220
		30	13,3	6,2	9,4	13,3	26,9	15,5	37,2	63,1	1,280
		100	6,7	4,7	6,9	10,4	23,9	11,2	40,8	64,6	1,310

1.7 Summary

Experimental methodology was developed, and repeatability analysis was conducted. The effect of nozzle orientation was determined and spray analysis using urea-water solution for the heated nozzle system. Different parameters were tested, such as mass flow rate and distance from the nozzle.

2. Numerical Modelling of the Heated Nozzle

The measurements of Chapter 1 were used to develop a 3D CFD simulation model capable of replicating the spray characteristics of the heated nozzle.

ANSYS FLUENT 2020R2 was used to perform the simulations. The simulation work was carried out in Euler-Lagrangian framework, where the quiescent conditions were represented by Eulerian phase and the droplets were resolved in Lagrangian phase. A simple cylindrical geometry of 300 mm of diameter and 500 mm of length was selected to represent the continuous phase. Polyhedral mesh was used for domain discretization (FIGURE 7) and the droplets were injected into the domain using Rosin-Rammler parameters derived from the experimental work. Parameters like spray cone angle, initial velocity etc. were also extracted from experimental data. Three planes were set up (similar to the experimental mesh planes) as can be seen in FIGURE 8.

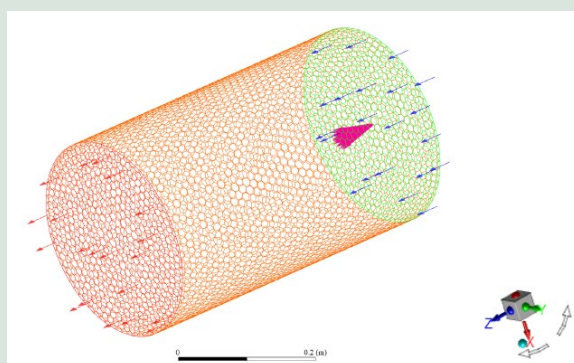


FIGURE 7. Mesh geometry.

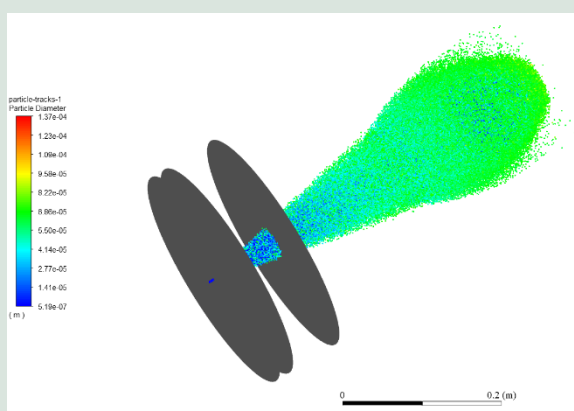


FIGURE 8. Simulation of the spray with the three planes $Z=10, 30$ and 100 mm.

2.1 Determination of the Cone Angle

Cone angle of the spray was determined for 500 g/h of mass flow set point with the measurement file 'NC_CentrePlane_UWS_500gmhr-301C_CAP-mod'. The measurement was recorded in terms of a centre plane forming a triangle away from the nozzle tip in the Z-direction in terms of count rate.

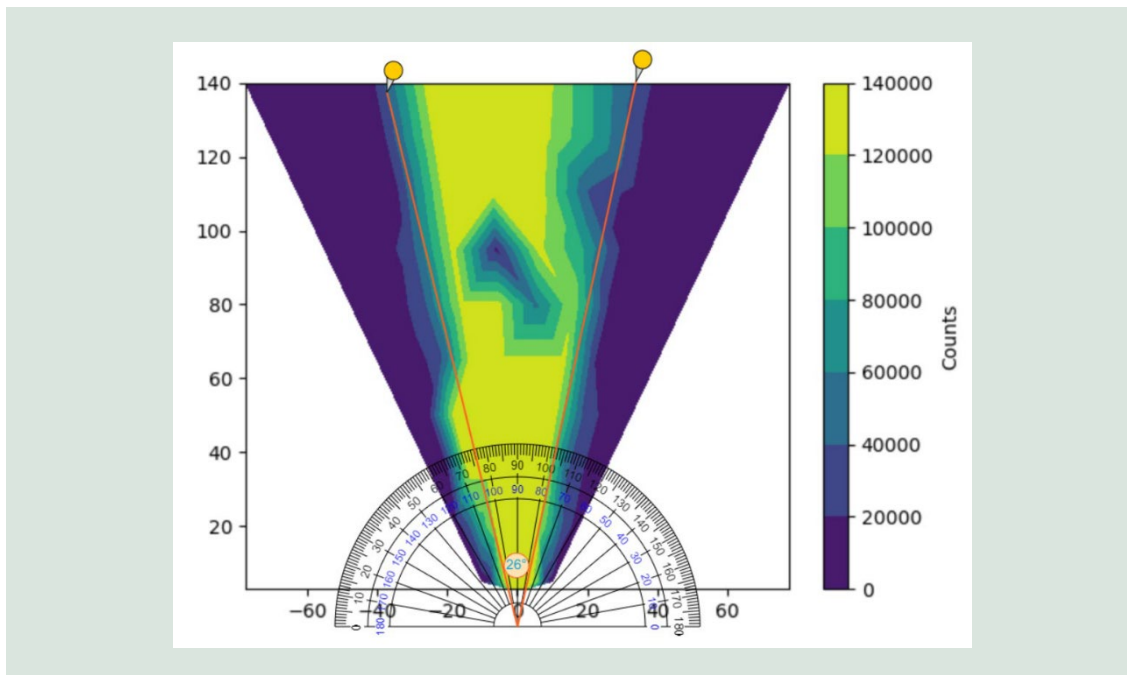


FIGURE 9. Spray angle taken from measurement data.

As there was just a single flow rate measurement available to determine a cone angle, a moderate approach was taken to accommodate this cone angle for both high and low flow rates. The result is shown in FIGURE 9. **Fejl! Henvisningskilde ikke fundet.**

2.2 Determination of Initial Velocity

It was particularly important to determine the correct initial velocity for the droplet distribution in this type of spray as the droplets were very small and there could be a dramatic change in the velocity downstream the nozzle tip. Therefore, the center plane measurement 'NC_CentrePlane_UWS_500gmhr-301C_CAP-mod' was utilized. A 2 mm diameter from the center line was placed along the Z-direction to calculate the average droplet velocity along the center line. Since PDA could not measure the exact droplet velocity at the nozzle tip, a backward linear fitted curve was then used to determine the velocity of the particles exiting the nozzle as also explained in (Khan, 2022). The result is shown in FIGURE 10. **Fejl! Henvisningskilde ikke fundet.**

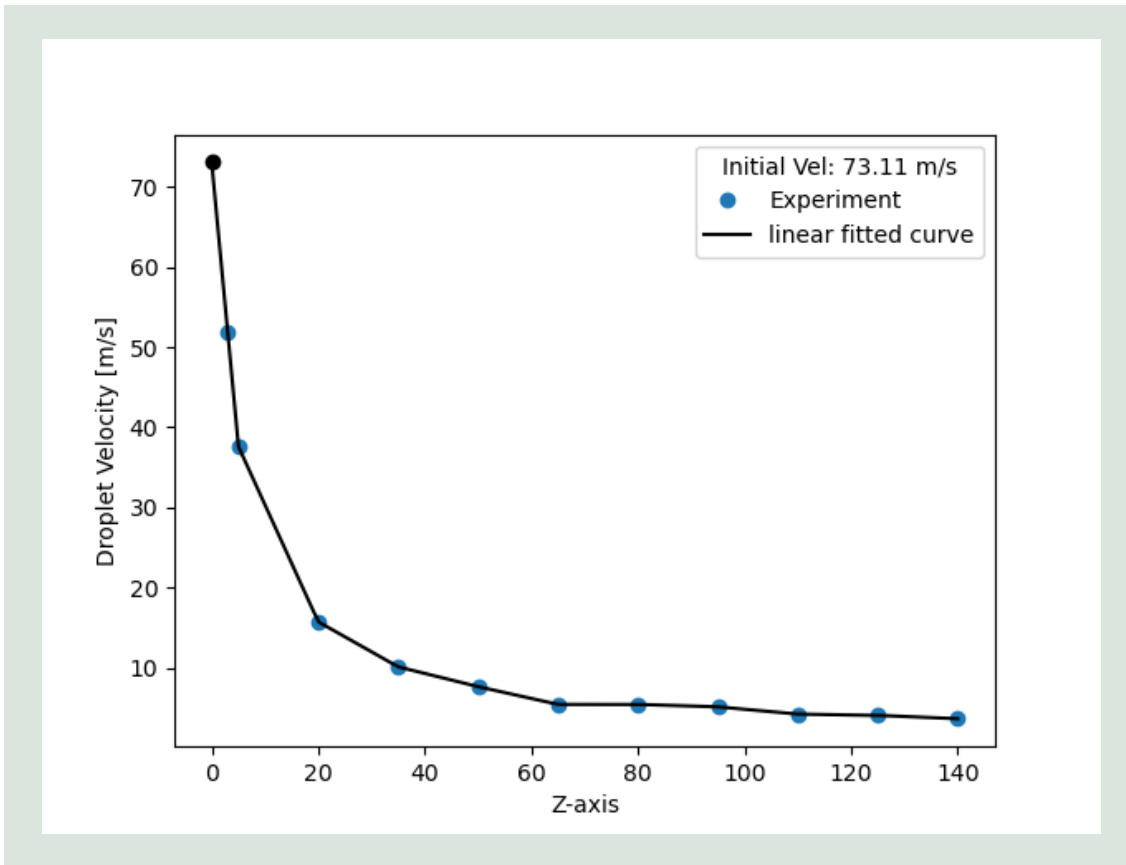


FIGURE 10. Estimation of initial velocity of the droplets.

2.3 Validation and Results

The results from simulation were validated against the experimental data in terms of planes and can be seen from FIGURE 11. It was observed that the cumulative distributions in the simulations correspond well with the experimental data with the trend becoming more prominent as the mass flow rate increases.

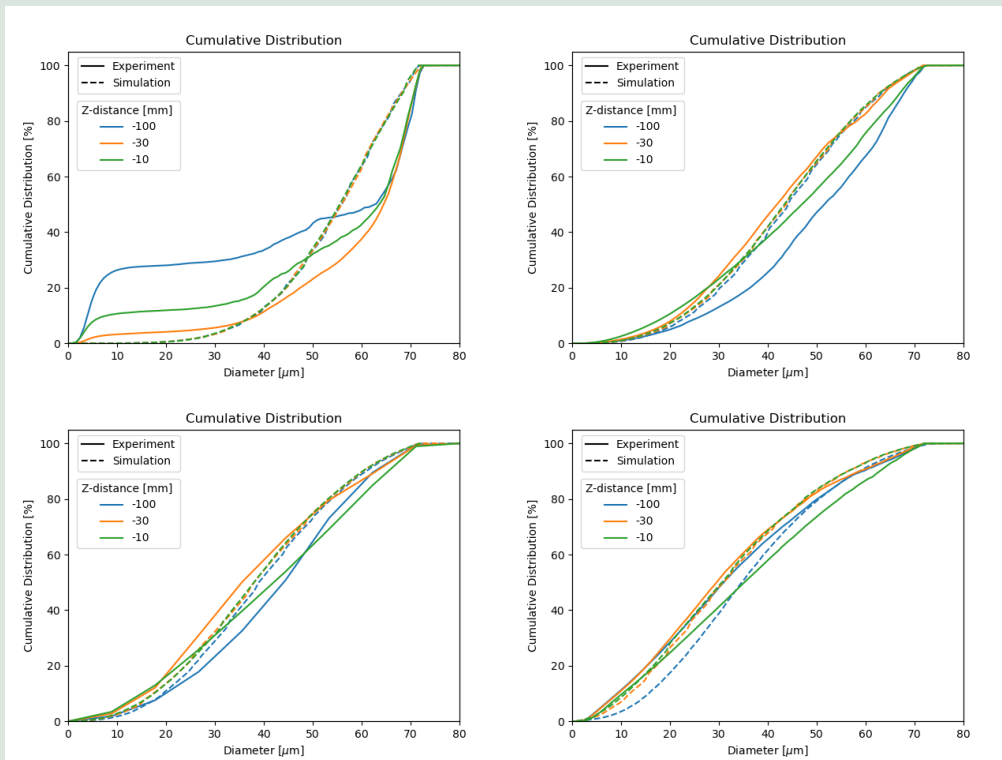


FIGURE 11. Validation results: Top left: 100 g/h, top right: 350 g/h, bottom left: 500 g/h and bottom right: 1000 g/h.

2.4 Summary

A good correlation has been seen with the experiments, with the validation improving with an increase in mass flow rates.

3. Development of Full Aftertreatment System

The simulation model of Chapter 2 is adapted to the commercial CFD software used by Dinex for the application to a full-scale exhaust gas aftertreatment system.

3.1 Adaptation and application of the heated nozzle CFD model

The heated nozzle CFD model was transferred from ANSYS Fluent 2020R2 to AVL Fire R2022 for application in the full exhaust gas aftertreatment system. Some changes were made to improve correlation and to make the model fit for AVL Fire. The changes are outlined in TABLE 3 below.

TABLE 3. Spray model adaptation in AVL Fire

Initial velocity	The model was manually adjusted to achieve a better fit with experiments
Initial temperature	Instead of applying the set point temperature, the initial temperature was based on a measurement inside the nozzle (effectively lowering the medium temperature)
Droplet size distribution	Instead of a Rosin-Rammler approximated distribution, the actual measured distribution in the first measurement plane (Z=10mm) was applied

The correlation between simulated and tested initial velocities can be seen in FIGURE 12.

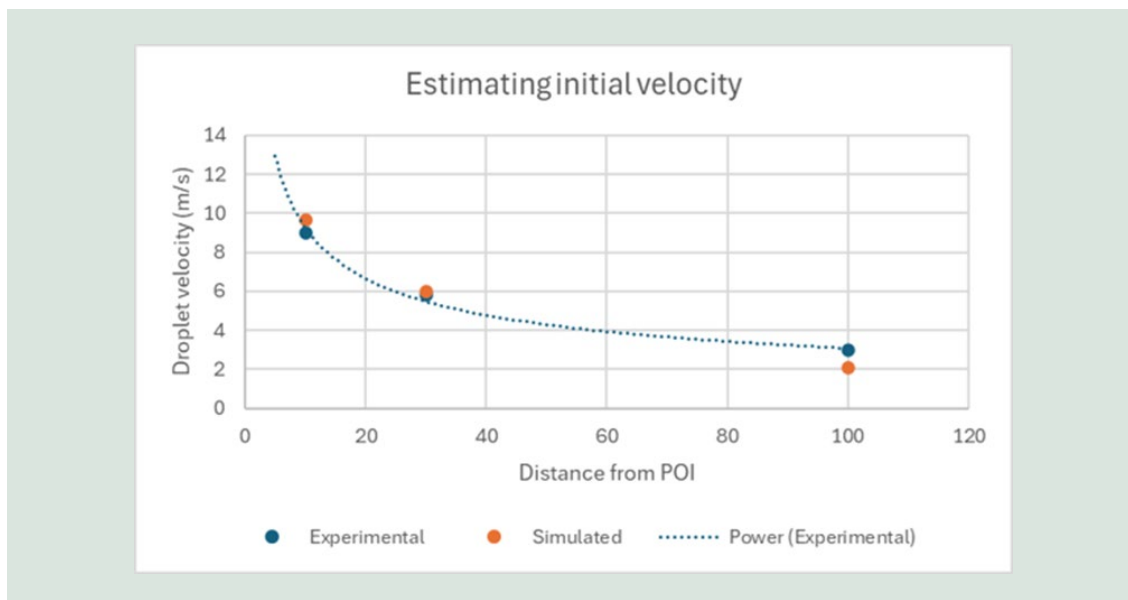


FIGURE 12. Comparison between simulated and measured droplet velocities in the 3 planes (10, 30 and 100mm).

Similarly, the measured medium temperature at varying mass flow rates can be seen in FIGURE 13. **Fejl! Henvisningskilde ikke fundet..**

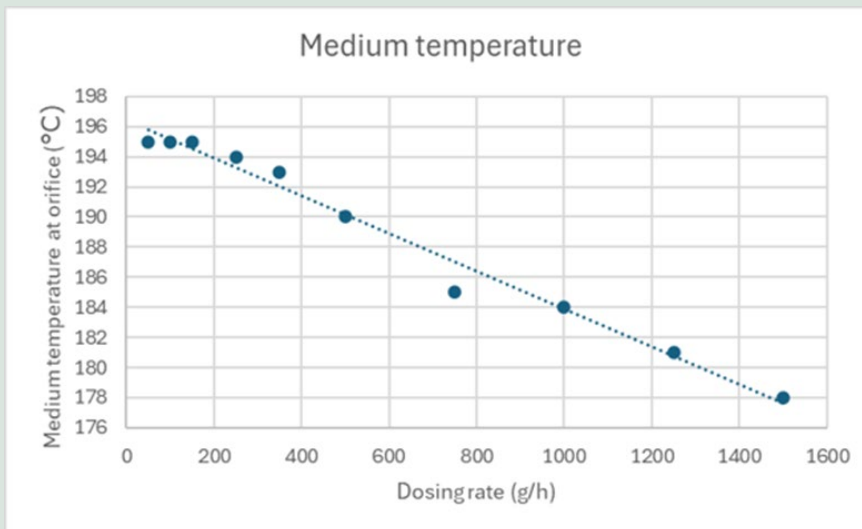


FIGURE 13. Measured medium temperature used as starting temperature for simulations.

3.2 Heated nozzle simulation results and calibration (sub model)

After running the initial heated nozzle simulations, the result was compared to test data – specifically the Sauter-mean-diameter in the 3 planes introduced in Chapters 1 and 2. The comparative results can be seen in FIGURE 14.

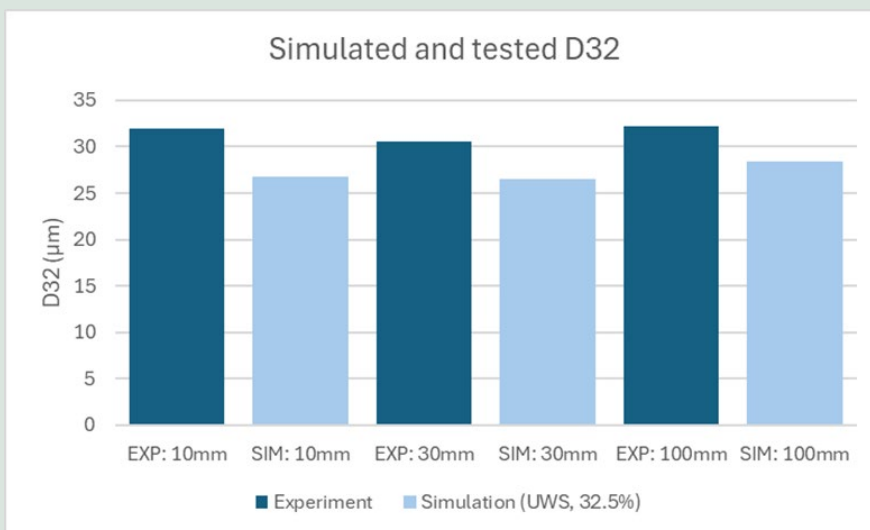


FIGURE 14. Comparison of characteristic droplet sizes (D32, Sauter-mean-diameter) between experiment and simulation.

It is seen that the droplet sizes are generally underpredicted. This prompted an investigation into plausible causes. It was discovered that if the composition of the liquid phase was altered such as to be more saturated (i.e. higher urea fraction) the droplet size distribution would remain much closer to the measurement, this is ascribed to the fact that urea has a much higher evaporation point than water. Observing the actual dosing, it can also be clearly seen that some quantity of the liquid is vaporised (what looks like smoke is expelled from the orifice). It is known from literature (Nishad, et al., 2019) that the water is evaporated first, and urea is

subsequently decomposed. This further supports and validates the hypothesis that actual urea concentration in the droplet is different from the 32.5% present in AdBlue. This led to the revised spray conditions for the simulation as described in TABLE 4. **Fejl! Henvisningskilde ikke fundet..**

TABLE 4. Revised spray model.

Liquid phase	
Initial velocity	As calibration shown in FIGURE 10. Fejl! Henvisningskilde ikke fundet.
Spray cone angle	As described in Determination of the Cone Angle
Initial temperature	According to in-nozzle measurements as shown in FIGURE 13. Fejl! Henvisningskilde ikke fundet.
Droplet size distribution	From PDA measurements
Chemical composition	Pure urea
Vapor	
Initial velocity	As liquid phase
Initial temperature	As liquid phase
Droplet size distribution	Initiated as "pure jet", essentially immediate, complete evaporation upon entry in the domain
Composition	Pure water

This resulted in the comparative results shown in FIGURE 15. Comparison of characteristic droplet sizes (D32, Sauter-mean-diameter) between experiment and simulation with revised spray settings as in TABLE 4. **Fejl! Henvisningskilde ikke fundet..** It is seen that the Sauter-mean-diameter has increase (orange bar vs light blue) resulting in a droplet size distribution, much more comparable to the experiment (dark blue).

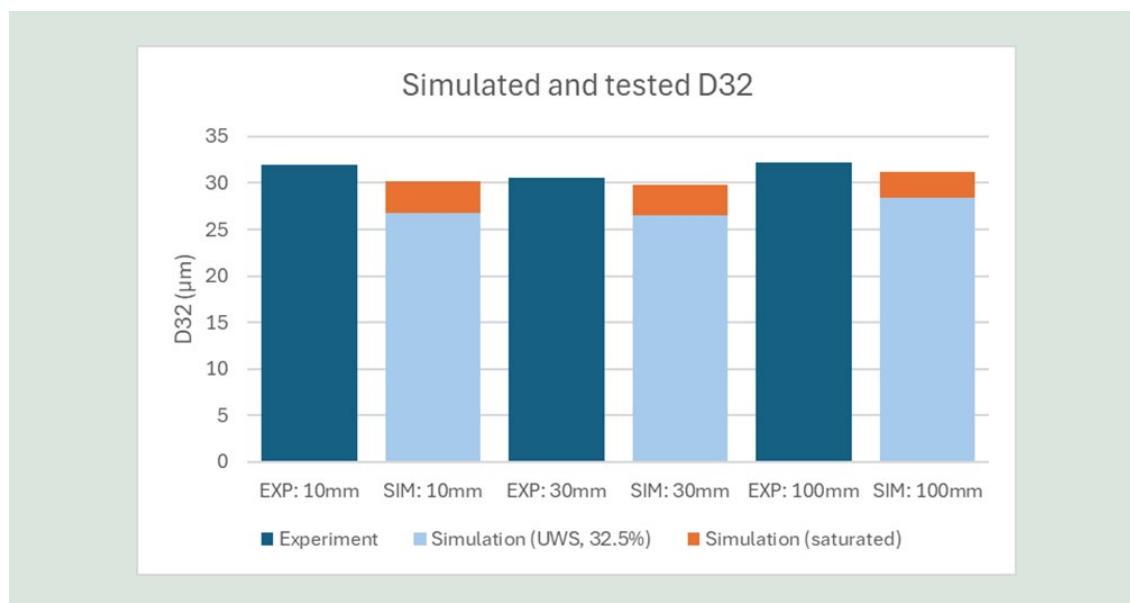


FIGURE 15. Comparison of characteristic droplet sizes (D32, Sauter-mean-diameter) between experiment and simulation with revised spray settings as in TABLE 4.

3.3 Model Validation

The spray model as described in section 3.2 and specifically TABLE 4. Revised spray model. was applied to simulation framework as described in (Bebe & Andersen, 2020). The geometry on which the simulation was performed were also like that of (Bebe & Andersen, 2020).

3.3.1 NH3 Uniformity

The first characteristic that was compared was the distribution of NH3 on the catalyst front face, in measurements this is assumed to be analogous to NOx reduced after the SCR, as described in more detail in (Bebe & Andersen, 2020). In FIGURE 16 a visual representation of the distribution can be seen, it is observed that general trends are captured, i.e. relatively higher concentration zone “1” compared to a relative low concentration zone “2”.

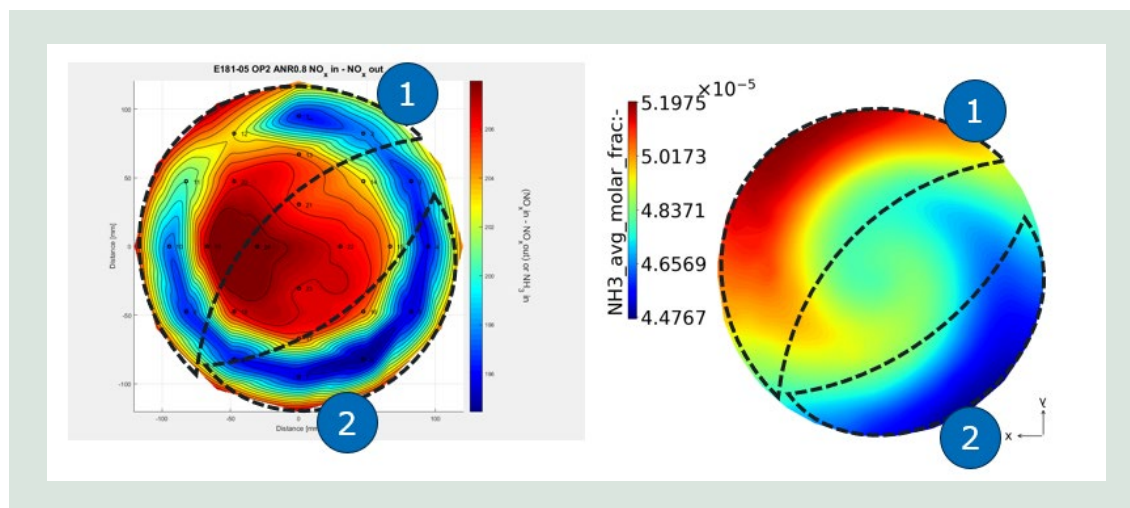


FIGURE 16. Side-to-side view of concentration colour plots. Left hand side is test while right hand side is simulated.

The comparative calculated uniformity indices of the tested and simulated distributions are listed in TABLE 5. The difference between the two is less than 1%.

TABLE 5. Calculated uniformity indices of from test and simulated distributions.

Tested	Simulated
0.989	0.985

3.3.2 Spray Propagation

To enable evaluation of the spray propagation inside a mixing geometry at actual operating conditions, it was decided to perform a 1-hour stationary test in an overdosing condition, to provoke urea deposition that would allow a qualitative analysis of the approximate impingement point. FIGURE 17 (top) shows endoscope photos captured inside the mixer after completion of the test alongside a graphical indication of the deposition of the deposit position, while FIGURE 17 (bottom) shows a side-to-side comparison of graphical indication of the deposition of the deposit position on a CAD (top) and the corresponding picture from the simulation (bottom) showing in blue the impingement area of the spray on the wall.

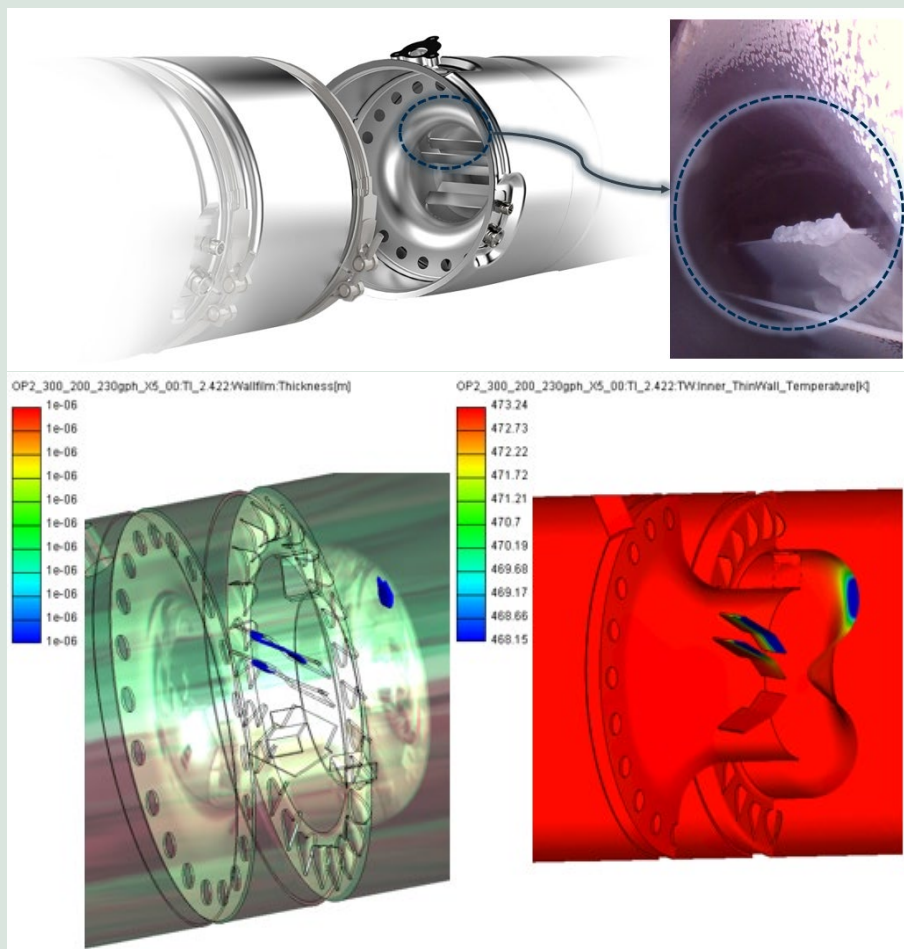


FIGURE 17. Spray impingement area, comparison between test (top) and simulation (bottom).

3.4 Mixer Development

The overall development procedure and workflow remains as described in detail in (Bebe & Andersen, 2020). However, to suit this spray technology better, the design philosophy applied has changed, illustrated in FIGURE 18.

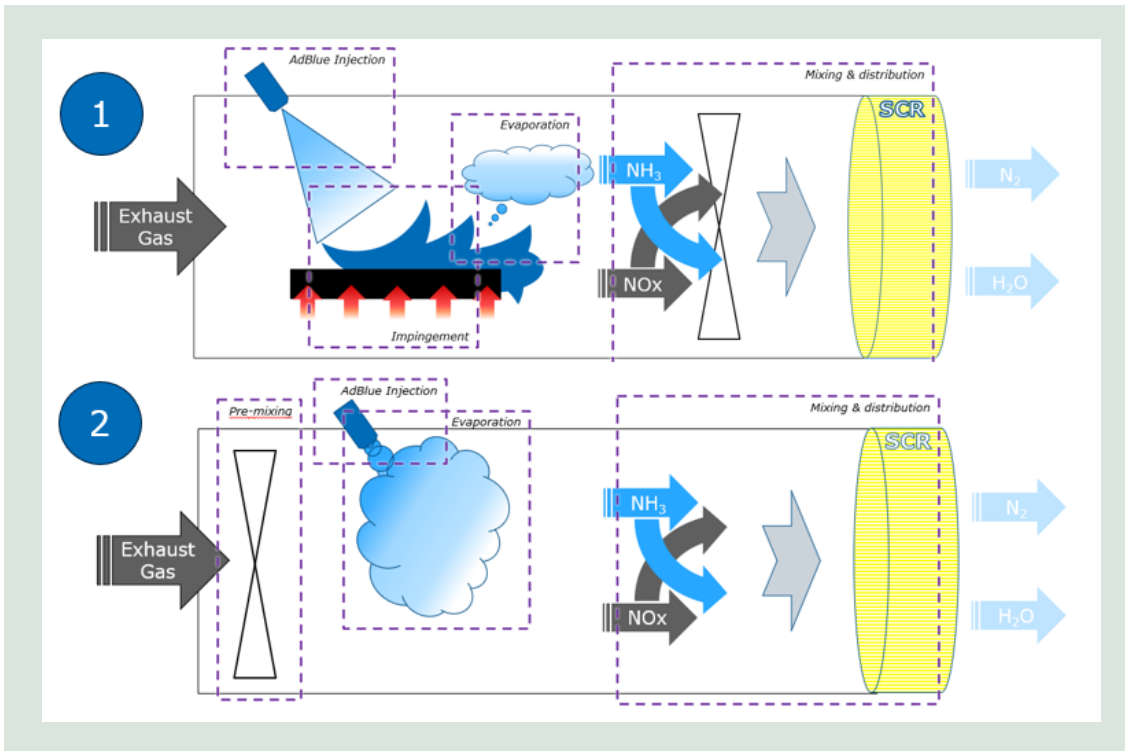


FIGURE 18. Design philosophies, baseline (1), top and for heated nozzle (2), bottom

Furthermore, during the evolution of the project, it became apparent that the market had more interest in reducing the space claim of a mixer fitted with a heated injection system, therefore the reduction in space claim has been deemed more important than pressure drop. An example of a typical aftertreatment system of the future was presented at the ECT Conference in 2023 (Wolff & Pfeiffer, 2023).

3.4.1 Performance

The mixer performance characteristics has been evaluated according to the typically applied methodology (also described in (Bebe & Andersen, 2020)).

An exemplification of the simulated uniformity index of flow and NH3 can be seen in FIGURE 19. **Fejl! Henvissningskilde ikke fundet..**

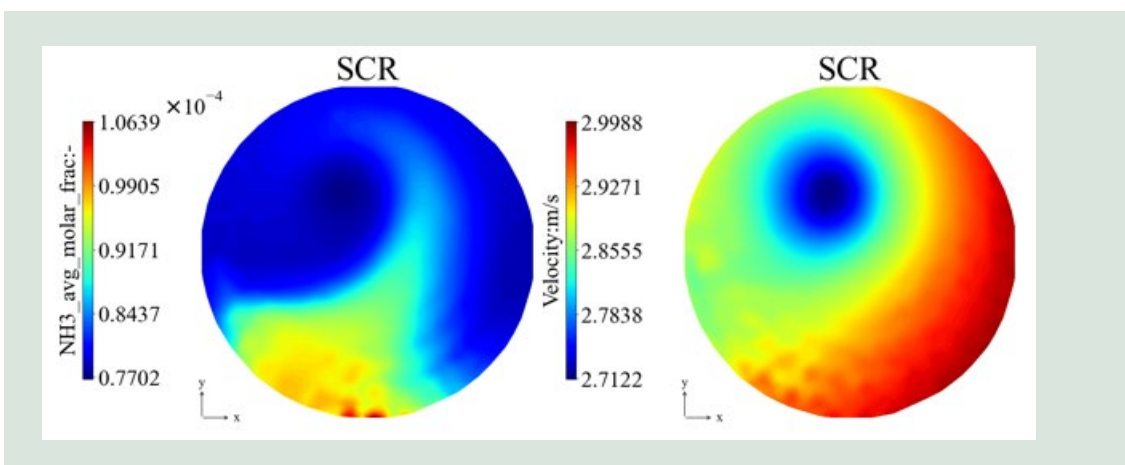


FIGURE 19. Example of simulated distributions of NH3 and flow on the SCR inlet face.

The uniformity indices calculated from the simulations depicted above is shown in TABLE 6. **Fejl! Henvissningskilde ikke fundet..**

TABLE 6. Uniformity indices calculated from the simulations

Mass flow rate	Temperature	NH3 UI	Flow UI	Pressure drop
300 kg/h	200 °C	0.97	0.99	1.72 kPa

In FIGURE 20FIGURE 15. Comparison of characteristic droplet sizes (D32, Sauter-mean-diameter) between experiment and simulation with revised spray settings as in TABLE 4. TABLE 1Fejl! Henvisningskilde ikke fundet., a comparison (in scale) between the space claim of the two mixers can be seen. It is clear, that the development for this work is significantly smaller and would be much more fit to be packaged in the available space close to an engine. The mixer remains scalable and can thus be made fit for different engine sizes.

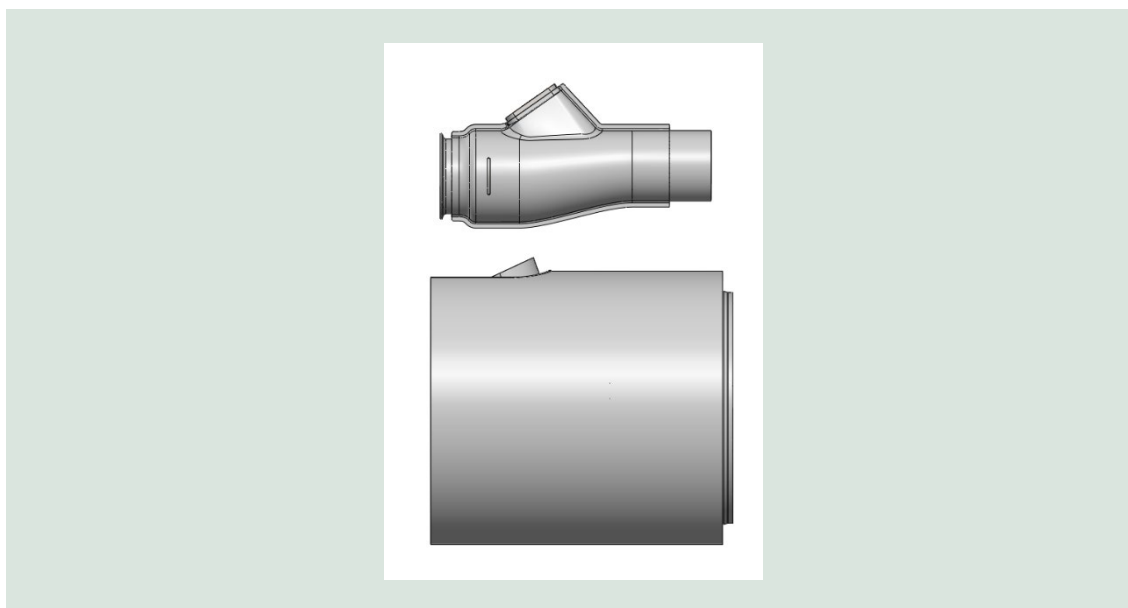


FIGURE 20. Scale comparison between benchmark mixer (top) and current development (bottom)

3.4.2 Durability

The durability of the mixer was validated using FEA (Finite Element Analysis), the simulations were performed on ANSYS Mechanical R2022, to the procedure and best practice as described in Chapter 4 of (Bebe & Andersen, 2020). The mixer has been considered fixed in an arbitrary pipe-routing somewhat representative of what could be expected in a real application. The pipe-routing with fixation points can be seen in FIGURE 21.



FIGURE 21. Boundary conditions and installation for FEA

It was found that the first 3 modes were all “body-modes” excited at the frequencies list in **Fejl! Henvisningskilde ikke fundet.**, for typical vehicular applications the first frequency should come beyond 25Hz, and typically eigenmodes up to 500Hz are identified.

TABLE 7. The first 3 eigenfrequencies

Mode no.	Frequency [Hz]
1	259.39
2	314.92
3	442.34

And an image depicting first mode can be seen in **FIGURE 22Fejl! Henvisningskilde ikke fundet.**

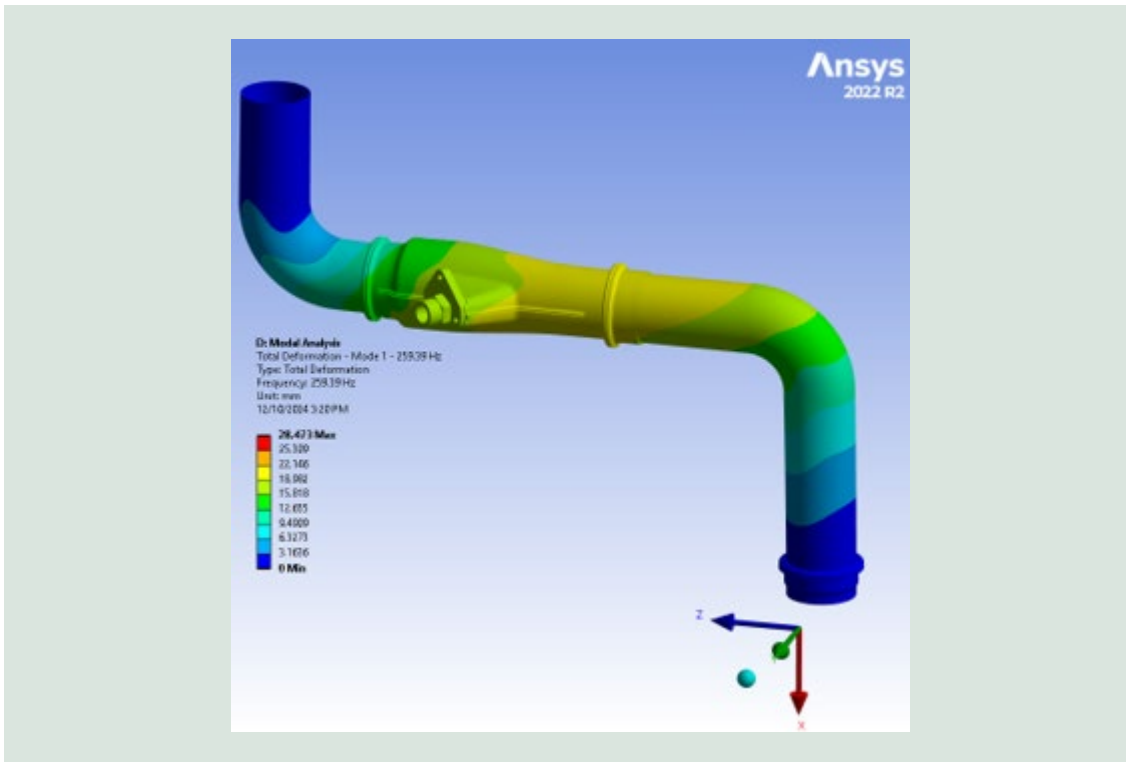


FIGURE 22. First mode shape of the mixer and pipe-routing.

The material data considered for the simulation can be viewed in TABLE 8. Note that material data has been considered at operating conditions for the mixer (400°C).

TABLE 8. Material data used for the structural simulation.

Material	Density	Young's Modulus	Poisson's Ratio	Yield Limit
AISI 441 (considered at 400°C)	7000 kg/m ³	1.85E+05 MPa	0.27	290 MPa

In conclusion, the mixer in the arbitrary pipe routing has first eigenfrequencies at frequencies much beyond what is typically expected in vehicular applications.

3.4.3 Manufacturability

The mixer will be constructed from 3 primary components: a body/housing a cone and a mixing device.

The body will be produced from deep drawn parts with secondary piercing and trimming operations.

The cone will be produced from a punched sheet metal part that will be subsequently rolled.

The mixing device can be made from pierced/laser cut parts for low volume – or from injection molding considering higher volumes.

The final assembly is done by welding, all components and subcomponents are largely fixed by poka-yoke and with easily readable features to indicate welding zones, examples indicated in FIGURE 23.

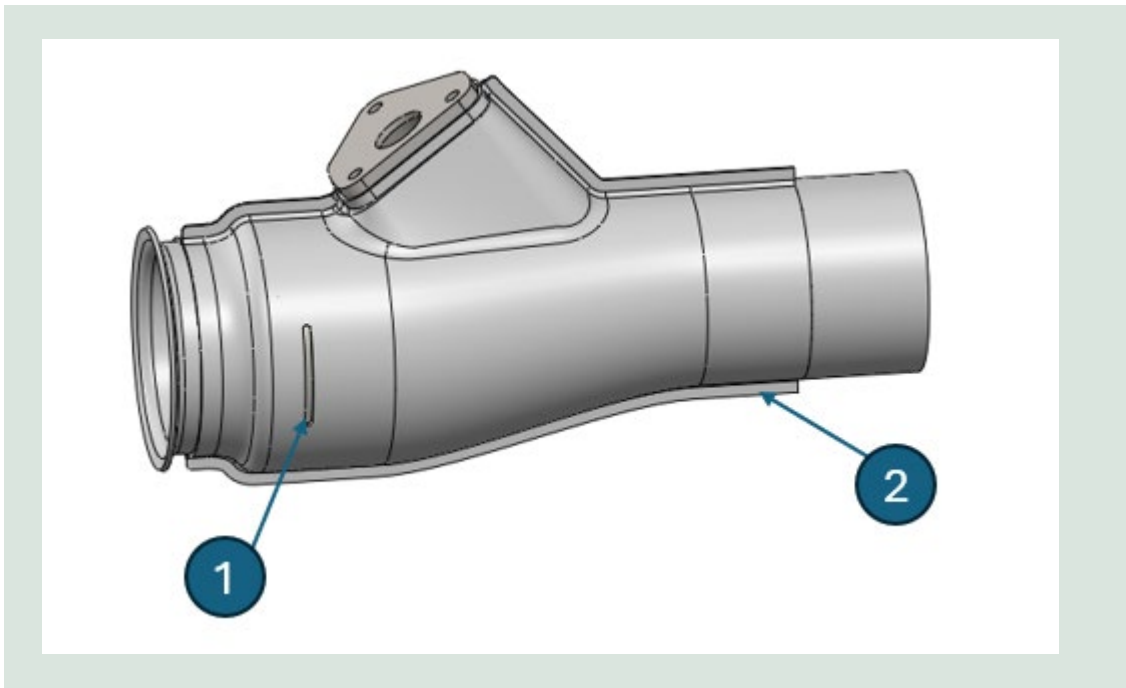


FIGURE 23. Figure indicating areas for welding.

3.5 Summary

In this chapter, the measures taken to improve the model for fitness to application in a full-scale exhaust gas aftertreatment system has been presented, along with some measures to further improve the fidelity. The simulation model has been applied to a benchmark mixer geometry to prove validity as well as to the development of a new mixing concept, which has proven to meet the targets for simulation (uniformity index of NH_3 exceeding 0.95). The mixer development of the current work has also been prepared in a way that makes it suitable for serial production, finally, using FEA, the mixer has also been simulated to ascertain that it meets basic durability requirements.

4. Software and Testing Support

A separate working package was planned to cover the necessary support and knowledge sharing, necessary to commission and successfully operate the novel technology. This chapter describes the key elements of the dosing system and their functionality.

4.1 Introduction and Working Principles of the Heated Nozzle

The so called “heated nozzle” is a device for injecting a urea water solution (UWS/AdBlue®/DEF) into the exhaust system of a commercial vehicle. It is operated without moving parts (passive nozzle), as the requested dosing amount is regulated by a high precision dosing pump. In comparison to common series UWS injectors, the heated nozzle contains a temperature sensor and a heating device to heat up the UWS while it is passing the nozzle.

In dependence of the dosing amount, the heating device is settled to a certain temperature (“SetPoint Temperature”) to enable a total evaporation of the water, already in the nozzle. As a result, the volume expands approximately thousand-fold and generates an impulse, that pushes the residual medium through the nozzle and triggers the spray formation.

As the water is brought into the gas phase, the urea is consequently heated up with the effect, that it's decomposition into intermediate products (e.g. isocyanic acid (HNCO)) and into ammonia (NH₃) is triggered by starting thermolysis and (partly) hydrolysis.

The working principle is shown in FIGURE 24. **Fejl! Henvisningskilde ikke fundet..**

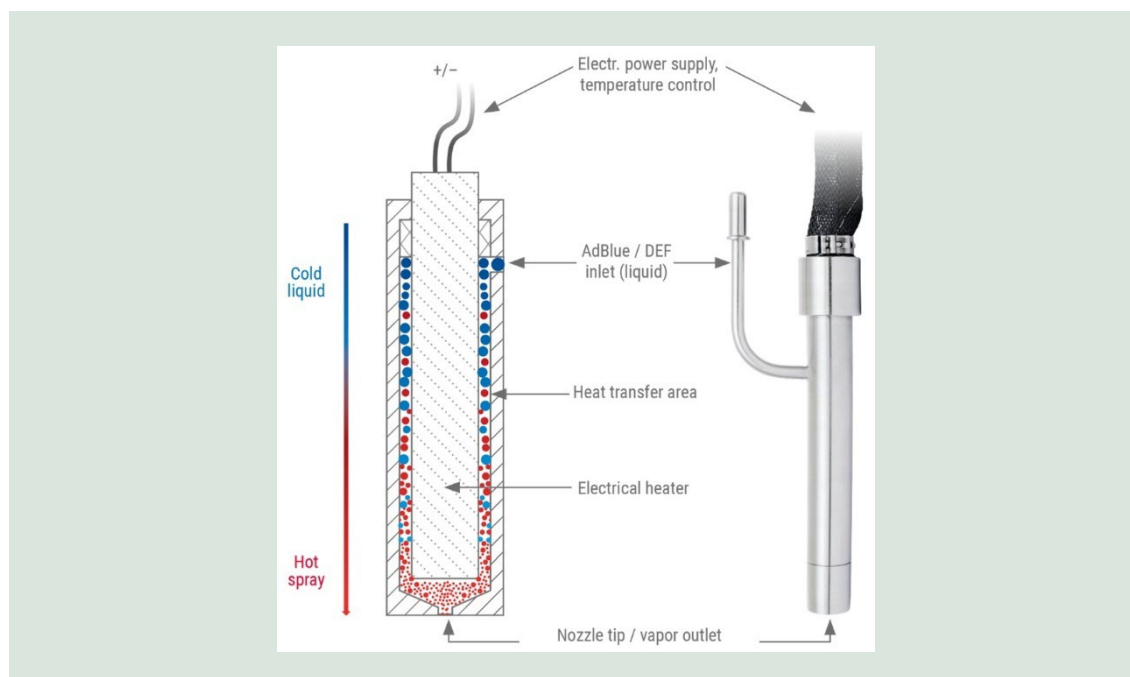


FIGURE 24. Working principle of Albonair heated nozzle.

4.2 Components of the Dosing System and Their Functionality

In the project “Development of an SCR system integrating a novel reductant delivery system” Albonair GmbH was responsible for building up, delivery and support of heated nozzle systems.

A heated nozzle system contains several instruments for a functional manner.

All parts and the functional principle of the heated nozzle, that are described before, are visualized in FIGURE 19. A dosing pump unit (containing a precision metering pump) regulates the requested dosing amount, and a purge box can be used for a cleaning routine, in which compressed air flows through the nozzle, blowing out all liquid and loose particle residues. In the current stage, the purge box is adopted for safety reasons, but this is not necessary during normal operations. An overview of the dosing system is shown in FIGURE 25.

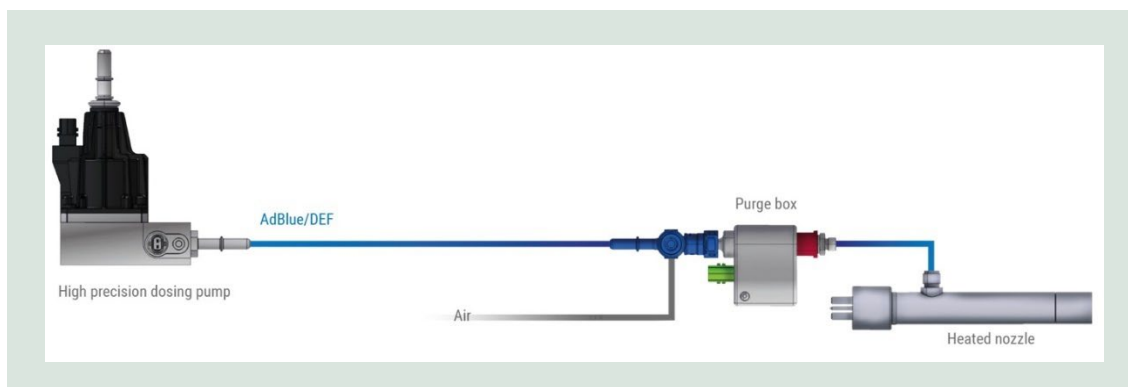


FIGURE 25. Components of heated nozzle dosing system.

4.3 Software and Controls

A controller is needed for dosing operation and regulation (not included in FIGURE 25). **Henvisningskilde ikke fundet.**

For controlling of the heating device, an additional controller and electrical supply unit were built up.

Both controller systems (dosing and heating) are finally integrated in their own software tool, that was programmed as an interface to the operator. Basic functions are the input and controlling of the dosing amounts, certain nozzle operating temperatures (“setpoint temperature”) and the data logging of the heated nozzle parameters.

Albonair built up all necessary parts and delivered them for this project: heated nozzle, Urea Dosing System (UDS) including metering pump, sensors, power supply and Aftertreatment Control Unit (ACU), wiring harness, pipes, hoses and the power supply with the temperature controller for the heating device of the nozzle. Besides that, all essential components for CAN communication were delivered. These components ensure a proper function of the system, and it could be integrated into the different test benches, especially the PDA tests setup and engine test bench.

Albonair developed the above-mentioned “Heated Nozzle Control Software” (HNC-SW, see FIGURE 26). **Henvisningskilde ikke fundet.** and delivered it, too.

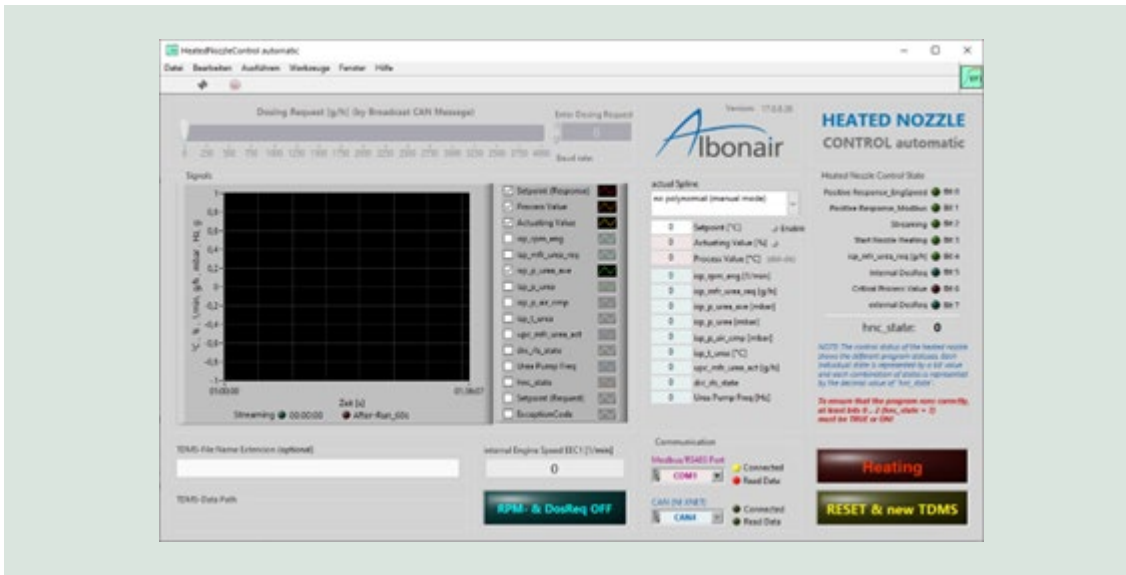


FIGURE 26. HNC software interface

All required documentation and instructions for using the software, installing the devices and application of the heated nozzle to engine exhaust pipe have been prepared and made available to the project partners.

4.4 Support During Project Execution

Albonair supported the tests and trials with one onsite visit and permanent remote support. Especially the data analysis of the heated nozzle's data recordings, their discussion and interpretation, but also of other recorded data (PDA, engine test bench) was undertaken as part of the work package of the present chapter.

5. Optimization of Prototype

In the initial phase of the project, all components for the heated nozzle system were planned, assembled/programmed and tested at Albonair. The heated nozzle, the dosing system and the HNC-Software were optimized during the execution of the project based on the data generated and observations.

5.1 Optimizations Due to Market Demand

The first sample of the dosing system contained a prototype of heated nozzle, that was equipped with a standard heating cartridge. It only could be operated with an electrical voltage of 44V, what is not applicable to the electrical system of a commercial vehicle with a common voltage of 24V.

In view of the intended application of the system for the exhaust gas aftertreatment of commercial vehicles, a second series of prototypes was constructed (see FIGURE 27 **Fejl! Henvisningskilde ikke fundet.**). The design of the heated nozzle was not changed, but a new heater was applied. It now is operated at 24V and has an electrical power of 1,5kW. The heating device is specially built for usage in the heated nozzle and consists of an exclusively designed heating wire. As a special feature, the nozzle was designed so that the nozzle tip can be changed with different geometries (e.g. bore for injection). These nozzles were named with the prefix "EICH".

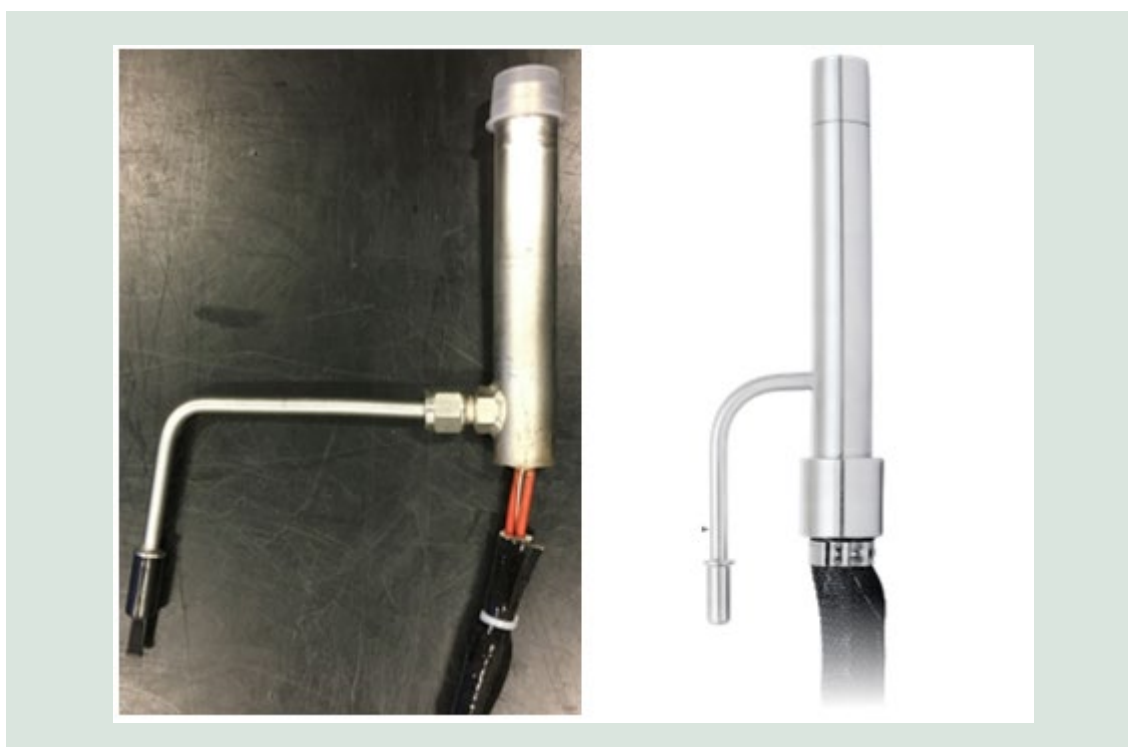


FIGURE 27. First prototype of heated nozzle (left) and the revised prototype "EICH" (right).

5.2 Geometrical (Design) Optimization

During the measurements with the PDA-System for the evaluation of droplet velocities and droplet sizes, the nozzle was mounted upwards at a 45° angle, and it was found that sometimes liquid urea accumulates on the nozzle tip at the outer rim. Consequently, urea could drip down from the nozzle and build solid residues, or the nozzle could be blocked in the nozzle tip, when the urea is cooled down (e.g. system shutdown). For a counter measure, a different design of the nozzle tip was intended, with a rounded shape of the nozzle tip, without any rim. FIGURE 28 shows on the left side the original nozzle tip design with a urea puddle on the top during the PDA measurements, while the new design is shown on the right side.

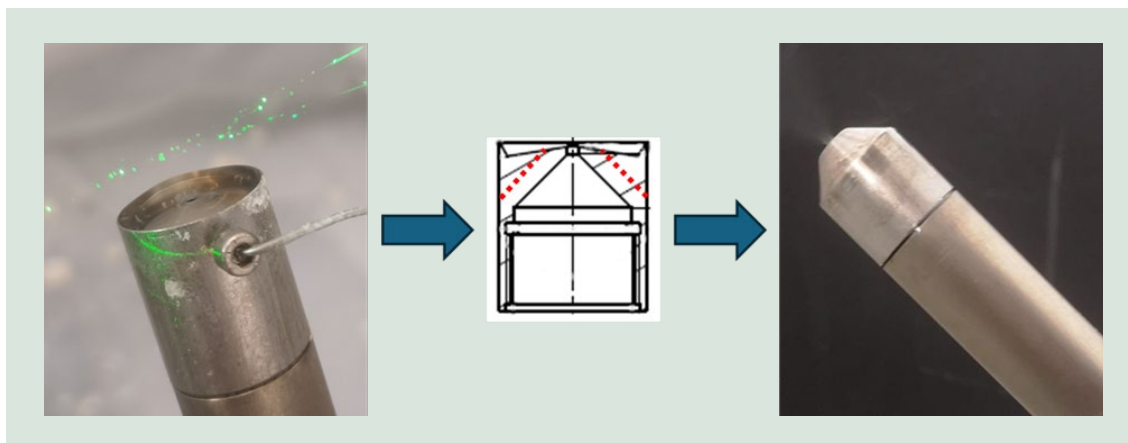


FIGURE 28. Different nozzle tip designs for spray optimization and to limit risk of deposition.

5.3 NH₃ Conversion Optimization

temperature level (>130°C) is required in the heated nozzle to start thermolysis and partial hydrolysis. On the other hand, the temperature should not be increased indefinitely, as a higher temperature also increases the risk of solid deposits. Besides this, the optimal nozzle operating temperature allows energy efficient operation, which in the case of commercial vehicle usage means lower fuel consumption and less CO₂ production. All this results in an operating temperature that depends on the current requested dosing amount. To operate the heated nozzle in this manner, Albonair established individual “heating curves” for each tested nozzle. FIGURE 29 **Fejl! Henvisningskilde ikke fundet.** illustrates the relationship between the required operating temperature (“SetPoint”) and the dosing rate, with the blue line representing the former. The dashed red line represents the temperature measured inside the nozzle cap and is consistently above the target temperature of 130 C for the conversion of NH₃.

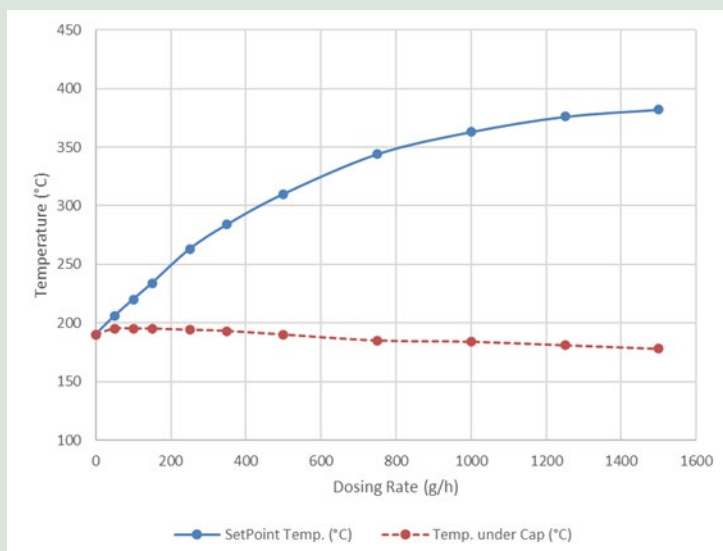


FIGURE 29. Heating curve (blue) of the heated nozzle and resulting temperature (red, dashed).

5.4 Controls Improvement

In an early HNC-Software version, the targeted operating temperature had to be entered manually into the controller device. This methodology was found to be suboptimal and disadvantageous when tested on the engine test bench, as it resulted in delays and only permitted the examination of stationary operating points.

For these reasons, the HNC-Software was improved, with an input area for the SetPoint temperature being integrated first. In addition, the required heating curves were implemented in the software. This enables the operator to either enter temperature specifications manually or to control the heating automatically based on the selected heating curve. This optimization also allows the heated nozzle system to be operated on automated engine test benches to proceed with transient test cycles, as the system can receive and process external dosing quantity requests via a CAN bus. The system is therefore able to react dynamically to incoming dosing requirements: The dosing system (UDS) converts the dosing quantities in real time, and, at the same time, the temperature is continuously adjusted to the boundary conditions. The HNC-Software automatically records and visualizes in real time parameters such as actual temperature, dosing quantity or dosing line pressure to monitor the operation at the test bench. The automated storage of this data enables detailed data analysis and postprocessing. As already explained, the efficiency of the conversion of urea into ammonia is sensitive to the operating temperature. To analyse the relationships and effects of the operating temperature on NH₃ production and NO_x reduction in an exhaust gas system, an offset function was also integrated to vary the setpoint temperature of the heating curve by a selected offset (max $\pm 10^{\circ}\text{C}$).

Using this software version, it was possible to operate the system automatically on the engine test bench, whereby the measurement data of the heated nozzle was recorded separately. Combining and analyzing the measurement data from the engine test bench with that from the heated nozzle was only possible through manual processing.

With the aim of simplifying and clarifying the data analysis, a further version of the HNC software included the transmission of internal parameters and measured values to the engine test bench system. The current version enables the complete integration of the heated nozzle system into the automation of the engine test bench. This includes the query of dosing quantities and the determination of corresponding target temperatures. In addition, all internal parame-

ters and measurement data are transmitted to the master system (engine test bench). As a result, all data is recorded and stored centrally, allowing a convenient data analysis and test evaluation.

6. System Validation

The nozzle with the improvements detailed in Chapters 4 and 5 is first used in conjunction with a baseline system, where performance is compared with a conventional, air-assisted nozzle. In a second step the heated nozzle is coupled to the mixer developed in Chapter 3 to undergo system validation on an engine dynamometer operated in realistic conditions, replicating actual vehicle use.

6.1 Benchmark Testing and Comparison to the Conventional Nozzle

A system using a mixer as the one developed in (Bebe & Andersen, 2020) was used as the EUVI reference benchmark system. On this system several tests were performed, namely:

1. NH₃ UI testing
2. Transient hot and cold cycles
3. Spray load study

The tests, except for the spray load study, was conducted with both the heated nozzle and a conventional air-assisted nozzle. The results and tests are summarized in the subsequent subsections. The test subject (system) installation can be seen in FIGURE 30. **Fejl! Henvisningskilde ikke fundet.**



FIGURE 30. Test setup for benchmark evaluation.

6.1.1 NH₃ UI Testing

NH₃ distribution testing was conducted with both the conventional, air assisted nozzle and the novel, heated nozzle. This was done to ensure that distribution did not play a decisive role in the evaluation of the emissions performance of the system with either nozzle. The NH₃ distribution measurement was also used for comparison to check the CFD simulation model. The

test is conducted according to the “24-point”-method, as also described in Chapter 4 of (Bebe & Andersen, 2020).

The results of an exemplary load point can be seen in FIGURE 31. **Fejl! Henvisningskilde ikke fundet..**

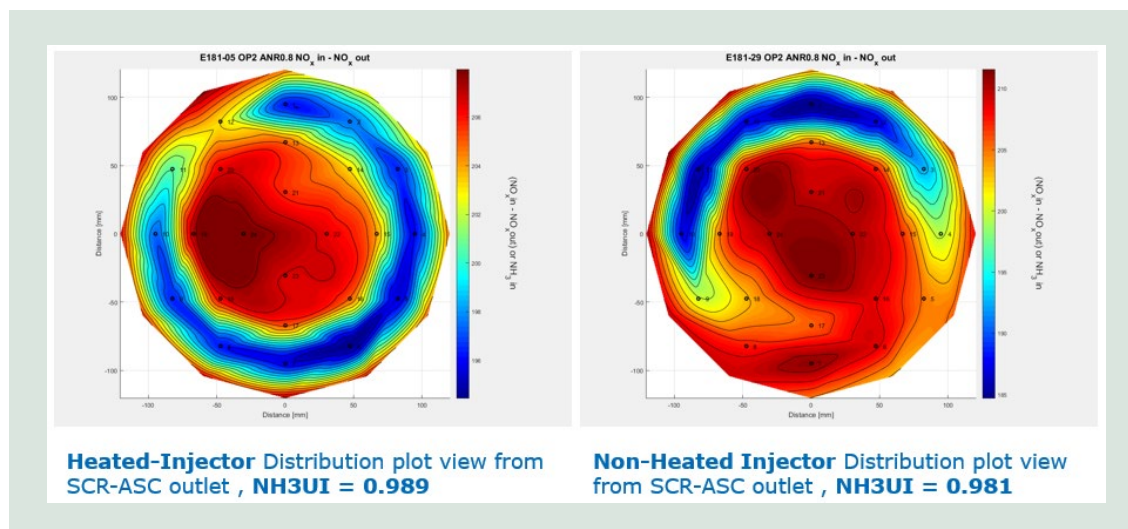


FIGURE 31. NH3 distribution results from engine dynamometer testing. The result corresponds to OP2, in TABLE 9)

The remaining UI results can be viewed in TABLE 9. **Fejl! Henvisningskilde ikke fundet..**

TABLE 9. NH3 distribution testing results from benchmark testing.

Operating point	Mass flow rate	Exhaust temperature	Heated nozzle UI	Conv. Nozzle UI
OP1	300 kg/h	250°C	0.990	0.989
OP2	300 kg/h	200°C	0.989	0.981
OP3	300 kg/h	300°C	0.978	0.990

The results show only a negligible difference, with the largest difference in OP3 where it was 1.2 percentage points.

6.1.2 Transient Hot- and Cold Cycle Testing

The transient tests have been performed on the industry standard “Nonroad Transient Cycle” (NRTC), the temperature and exhaust mass flow rate profile can be seen in FIGURE 32.

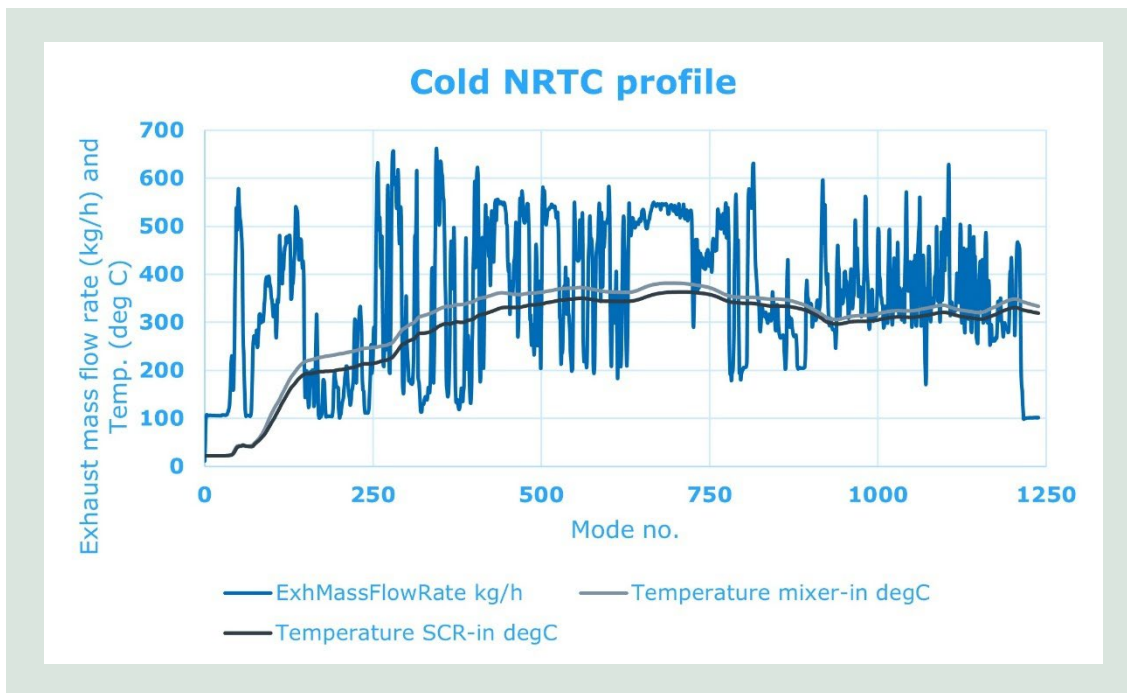


FIGURE 32. Cold NRTC profile

The reason for going for a nonroad rather than on-road cycle is primarily due to the relative interest of the non-road customers in the product compared to the on-road customers. The on-road segment has to a larger extent opted to go for exhaust gas heaters that has the added benefit of heating the catalyst quicker, albeit at the expense of requiring much more energy (electric power).

The results for a few exemplary cold cycles have been reported in TABLE 10TABLE 1Fejl!
Henvsningskilde ikke fundet., the variation shown is; 2 tests with the heated dosing unit and 2 tests with a conventional system, additionally there is a variation of ANR (Ammonia-to-NOx Ratio – a measure of the amount of AdBlue dosed, ANR=1.0, would signify a stoichiometric relationship between NOx and available NH₃ (from the AdBlue)). For all tests, a dosing release temperature of 180°C (average temperature between a temperature sensor sitting upstream and downstream the SCR catalyst) has been applied.

It is seen that engine performance is consistent across the different cycles, but it is also seen that dosing accuracy for the conventional nozzle used for benchmark is significantly worse than that of the heated dosing system. This makes it difficult to definitively conclude whether a performance benefit is observed if dosing inaccuracy is accounted for. The relative improvement does seem to be dependent on liquid flow rate (approximately 10% difference in cumulative NOx-reduction for the case run at ANR=0.6 and 13% difference in cumulative NOx reduction for the case run at ANR=1.0 and considering the dosing deviation of 4% and 7% respectively), this yields a performance improvement of about 6%.

TABLE 10. Exemplary cold cycle characteristics.

Test and injector	Engine work (kWh)	Cumulative raw NOx (g)	Cumulative NOx reduction (g/kWh)	Cyclic deNOx (%)	AdBlue consumed (g)	Dosing deviation from target (%)
Cold NRTC 0.6 ANR (Heated)	13.862	113.564	5.066	61.832	139.400	0.126
Cold NRTC 0.6 ANR (Conventional)	13.846	105.253	4.559	59.970	123.200	-4.363
Cold NRTC 1.0 ANR (Heated)	13.859	112.786	7.293	89.614	230.400	0.114

6.1.3 Transient Testing – Reduced Temperature Release

An important feature of the heated nozzle is the ability to start dosing AdBlue at lower temperatures than would normally be possible. A dosing release temperature of 180°C is on the limit of what will be possible in a conventional aftertreatment system. To evaluate the benefit of this feature, back-to-back testing was performed with 150°C and 180°C dosing release temperatures at an ANR=0.85. Considering the results shown in TABLE 10 **Fejl! Henvisningskilde ikke fundet.**, it was decided to perform both those tests with the heated nozzle. This would provide the most accurate dosing, and any added deNOx benefits of the heated dosing would be minor at best. The results of the cold NRTCs at these two dosing release temperatures is shown in TABLE 11 **Fejl! Henvisningskilde ikke fundet.** The time spend within dosing release conditions and the time gained for NOx conversion can be seen in FIGURE 33. Comparison of requested dosing and measured temperatures as indication of dosing release for the two cases of TABLE 11., where the temperature and the dosing request has been plotted in the same chart. When a certain temperature is reached, dosing release temperature is achieved. The time gained by lowering the release temperature was in this case 56 seconds.

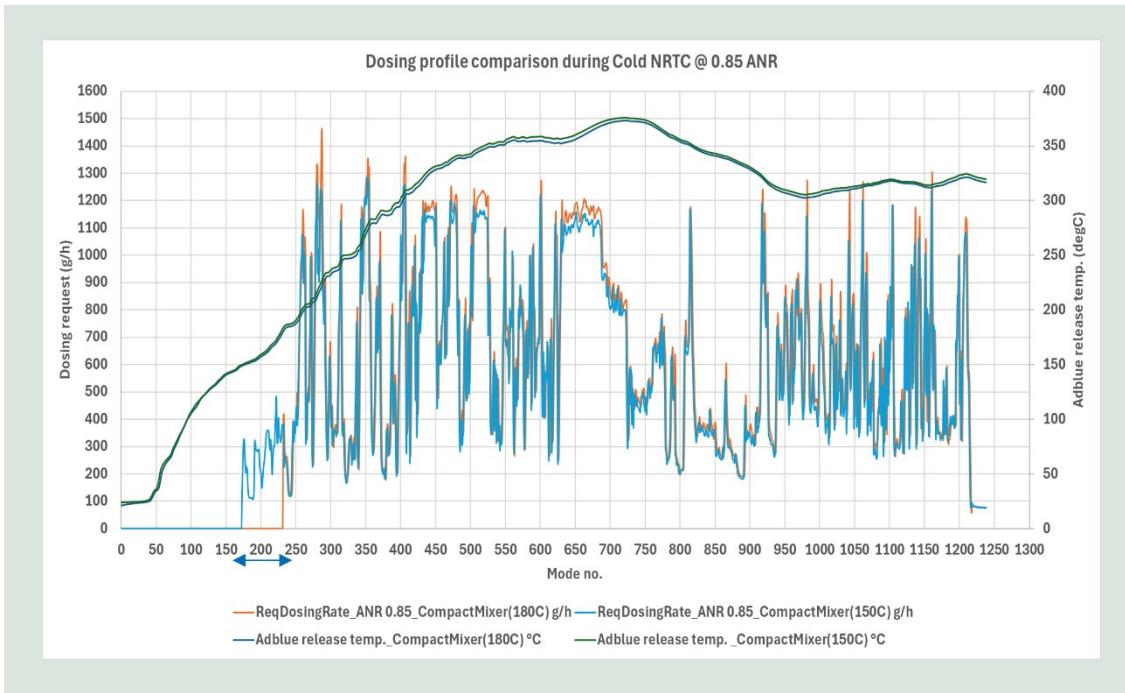


FIGURE 33. Comparison of requested dosing and measured temperatures as indication of dosing release for the two cases of TABLE 11.

TABLE 11. Comparison on cold NRTC 180°C compared to 150°C release temperature.

Test and injector	Engine work (kWh)	Cumulative raw NOx (g)	Cumulative NOx reduction (g/kWh)	Cyclic deNOx (%)	AdBlue consumed (g)	Dosing deviation from target (%)
Cold NRTC 0.85 ANR (180°C)	13.855	106.061	6.614	86.392	178.400	-0.607
Cold NRTC 0.85 ANR (150°C)	13.833	100.264	6.470	89.264	177.800	1.038

6.2 Bespoke Mixer Testing

This section will describe exemplary results of the validation activities performed on the bespoke mixer developed in Chapter **Fejl! Henvisningskilde ikke fundet.** considering the dosing system developed as part of Chapter **Fejl! Henvisningskilde ikke fundet.**

6.2.1 Prototyping and Installation

To replicate the intent of the serial design and the simulated models, a test setup was constructed with identical dimensions and layout. The mixer is produced as a one off from a combination of 3D printed parts (body/housing) and laser cut sheet metal components (internals). The parts are joined together by manual welding. The assembled mixer is mounted in an after-treatment system consisting of a DOC (diesel oxidation catalyst), a DPF (diesel particulate filter) intermediate piping and an SCR (Selective Catalytic Reduction catalyst). The test setup can be viewed in **FIGURE 34** **FIGURE 34.** Test setup on engine dynamometer with bespoke mixer. **Fejl! Henvisningskilde ikke fundet.**, note nozzle position is marked by the yellow circle. Before installed in the engine cell, the system is leakage tested.

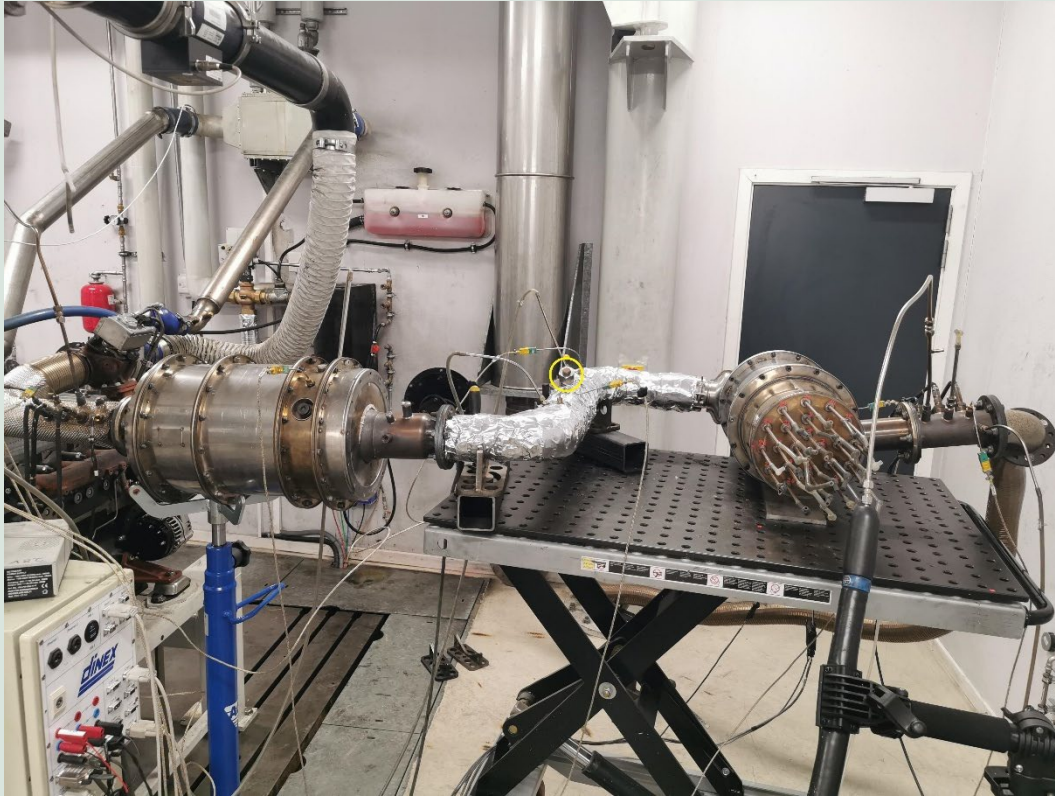


FIGURE 34. Test setup on engine dynamometer with bespoke mixer.

6.2.2 Backpressure Testing

The backpressure, or pressure drop test, is in Dinex a standardized 5-mode test, where absolute pressure is measured in different places throughout the exhaust system. The 5 modes are a composite of different engine speeds and torques, as shown in FIGURE 35. Henvissningskilde ikke fundet..

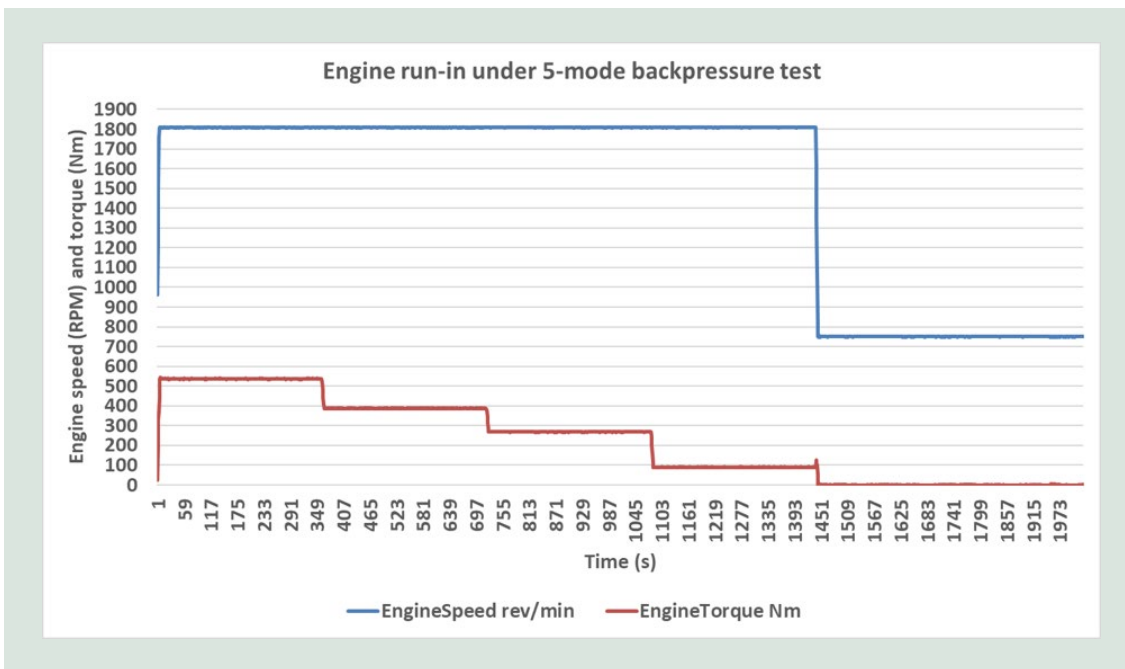


FIGURE 35. 5-mode pressure drop test.

The resulting measurements up- and downstream of the mixer can be seen in FIGURE 36. Pressure drops calculated from measurements up- and downstream of the mixer (blue) simulation results indicated with orange crosses. **Fejl! Henvisningskilde ikke fundet.** Blue points are measurements while the orange crosses indicate simulated pressure drops.

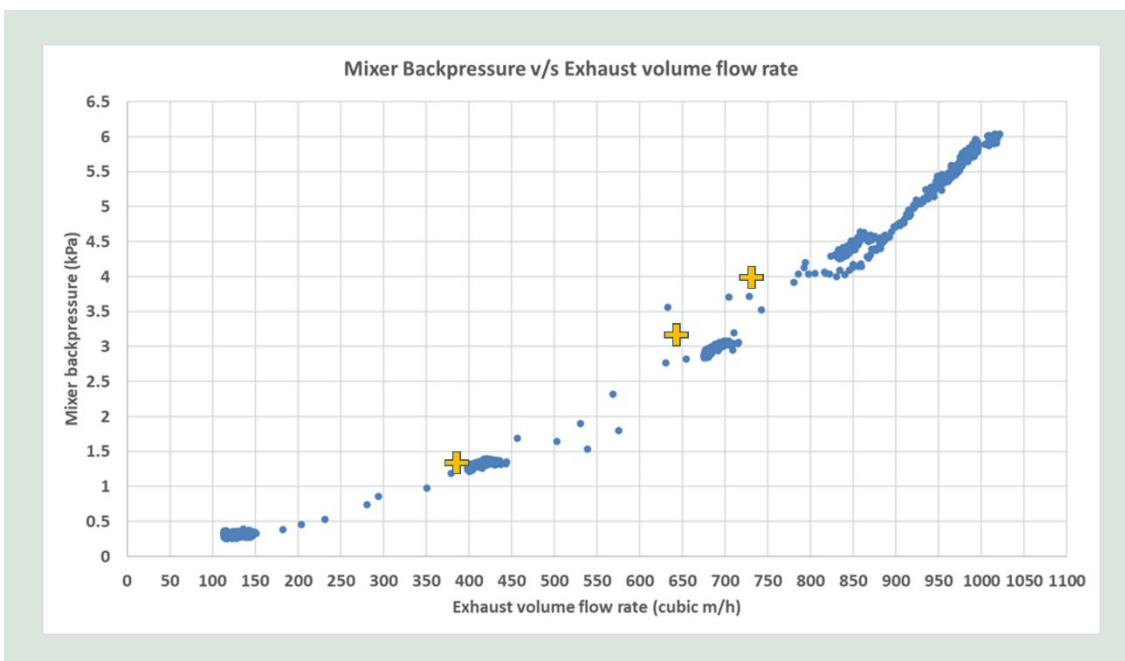


FIGURE 36. Pressure drops calculated from measurements up- and downstream of the mixer (blue) simulation results indicated with orange crosses.

6.2.3 Bespoke Mixer, NH3 UI Tests

In a similar fashion to what was described in Section 6.1.1 above, and in more detail in (Bebe & Andersen, 2020), uniformity was tested on the bespoke mixer as well. Compared to the initial testing, it was decided to choose a wider range of operating conditions, hence a difference

in operating conditions can be observed. In general, NH₃ distribution indices are high – also exceeding what was simulated. The results also appear reproducible based on two repeat measurements. A tabular overview of the results can be found in TABLE 12. **Henvissningskilde ikke fundet.**

TABLE 12. Bespoke mixer uniformity indices from test.

Operating point	Mass flow rate	Exhaust temperature	Heated nozzle UI 1 st test	Heated nozzle UI 2 nd test
OP1	300 kg/h	200°C	0.989	0.993
OP2	430 kg/h	300°C	0.997	0.996
OP3	250 kg/h	250°C	0.996	0.997

6.2.4 Deposit Testing

Testing was performed on the mixer in overdosing conditions, as described in Section 3.3.2, again, with the aim of evaluating the spray propagation. To compare with the CFD results of chapter 3. In FIGURE 37. **Henvissningskilde ikke fundet.** a comparison between test (left) and CFD (right) is shown. The CFD image shows in colour the steel temperature below a certain threshold. Blue is coldest, the mechanism is that steel temperature will drop upon impingement of liquid. On the left-hand side picture from test white deposition of urea is seen. While the point of impact is well aligned, test result does indicate that a larger proportion of the injected medium is spread beyond the spray cone defined from the lab test of Chapter 1.

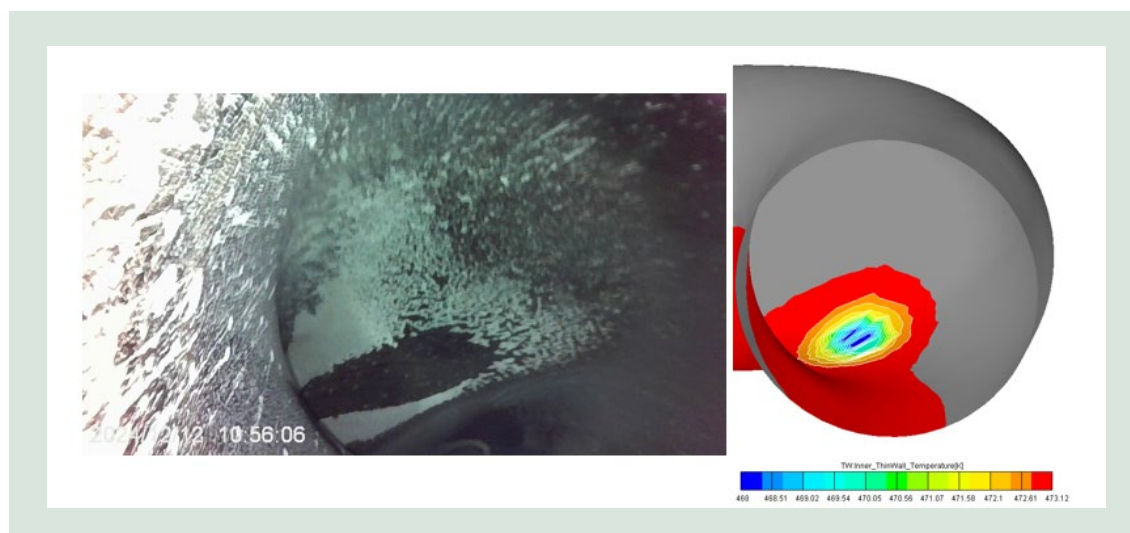


FIGURE 37. Comparison between test (left) and CFD (right) indicating spray propagation in overdosing conditions.

6.3 Discussion

With reference to the transient test comparison between the conventional and heated nozzle; It would be beneficial to increase the dosing accuracy for the conventional dosing system, this could be achieved by using improved hardware (specifically an improved pump). The result of this would be that it could be determined with great confidence whether a performance benefit is or isn't achieved with the heated nozzle.

Reflecting the correlation between simulation and testing, while benchmark testing on the baseline mixer as well as the correlation between lab testing and scale simulation was overall good, a larger discrepancy was observed for the bespoke mixer (especially on the NH₃ UI

testing). The fair correlation of pressure drop would indicate a good representation of the geometry in the prototype, while the spray load/deposit test does suggest that perhaps the spray cone angle is not sufficiently well described.

Results in TABLE 11 **Fejl! Henvisningskilde ikke fundet.** show that the time to start of dosing was significantly reduced when dosing release temperature was reduced to 150°C. This translates to an improvement in deNOx characteristics of the system, under the presented test conditions, the improvement is approximately 3%.

7. Dissemination

Throughout the project, the technology and its application to the aftertreatment systems of the future has been presented in industry forums as well as in meetings with current and potential customers in especially Europe and USA. This chapter describe some of the public presentations in more detail.

7.1 19th FAD-Conference “Challenge – Exhaust Aftertreatment”

In this conference, the heated nozzle was presented as an option for further lowering of NOx emissions to fulfil future emission legislations.

This presentation showed the working principle, objectives and possibilities of using the hot nozzle. First results of optical measurement techniques (Shadowgraphy and PDA) were shown, as well as the potential of nitrogen oxide reduction at low exhaust gas temperatures. The title of the presentation is: “Electrically heated nozzle for use at low exhaust gas temperatures to reduce NOx”.

7.2 IAA 2022

IAA is a tradeshow held bi-annually in Hannover, Germany. In 2022, the heated nozzle was presented in a separate part of the Dinex booth, with Albonair presenters assisting in presenting the technology to potential customers, a photograph from the exhibition at the booth can be seen in FIGURE 38. **Fejl! Henvisningskilde ikke fundet..**



FIGURE 38. Photograph of exhibition at IAA 2022.

7.3 ECT-2023 ECMA's 14th International Conference "Leaping to cleaner air for tomorrow"

In this conference, the heated nozzle was presented as part of a "holistic" view on the after-treatment systems of the future. At the conference, initial test results from the engine dynamometer were shown in a presentation called "Reaching EU7/BS7 emission limits for Commercial vehicles: a holistic approach by an exhaust aftertreatment system supplier".

7.4 AVL SIMpulse: Alternative Fuels for Internal Combustion Engines – Myth or Opportunity?

This online event series focuses on the application of simulation tools to the development of the mobility solutions of the future. In this event, Dinex participated with a presentation dubbed "3D CFD model development for a heated AdBlue dosing module and its application to H2 ICE aftertreatment". In which the application of the nozzle for aftertreatment systems for hydrogen internal combustion engines is explored. Data from both simulation and lab testing was presented.

7.5 Status at the Closure of the Project

Through the extensive testing a lot of knowledge and understanding has been garnered on the performance of the nozzle. Still a better understanding of the liquid thermal decomposition could be valuable, while attempts were made to model the flash boiling phenomena occurring in the nozzle, the very large gradients in fluid momentum and temperature rendered the attempts to simulate the process in CFD unsuccessful, and the composition of the resulting droplets (or particles) remain not definitively known. While good correlation on spray propagation between experiments and simulation was achieved, the deposition mechanism appears to be quite different for the heated dosing in comparison to conventional AdBlue dosing and needs also further dedicated studies to be better understood.

Commercially, there is still some uncertainty about the future regulations for the off-road sector, and the market is not yet confident what combination of technologies will be adopted for different applications.

8. References

- Bebe, J. E., & Andersen, K. S. (2020). *Kompakt mixer med lav termisk masse*. Miljøstyrelsen.
- Khan, D. B. (2022). Experimental Characterization and Numerical Modelling of Urea Water Solution Spray in High-Temperature Crossflow for Selective Catalytic Reduction Applications. *SAE International Journal of Sustainable Transportation, Energy, Environment, & Policy*, 3.
- Nishad, K., Stein, M., F, R., V, B., U, M., O, D., . . . A, S. (2019). Thermal Decomposition of a Single AdBlue® Droplet Including Wall–Film Formation in Turbulent Cross-Flow in an SCR System. *Internal Combustion Engines Improving Performance, Fuel Economy and Emissions*.
- Wolff, T., & Pfeiffer, M. (2023, Dehli). Reaching EU7/BS7 emission limits for Commercial vehicles: a holistic approach by an exhaust aftertreatment system supplier. *ECT International Conference*.

Development of an SCR system integrating a novel reductant delivery system

This multi-faceted project has had the overarching purpose of integrating a novel AdBlue dosing unit in a SCR system. The novelty of the dosing unit is connected to the device's ability to pre-heat the reductant prior to dosing it into the system. Owing to the multicomponent nature of the reductant, evaporation and thermal decomposition is not easily predicted. Therefore, substantial component testing has been performed with the aim of describing the characteristics of the dosed reductant.

As a second step, the characteristics defined from the laboratory testing has been used to develop a Computational Fluid Dynamics (CFD) spray model which could be applied for full system analysis for the development of a mixing system fit for the new dosing module type.

In parallel the dosing module has been further developed to achieve greater robustness in transient operation as well as in maximizing the amount of thermal energy the reductant can be exposed to, without risking failure caused by solid deposition of the urea byproducts well known in the field of urea-SCR-systems.

Finally, a bespoke mixing system was proposed based on the learnings of the project. On this, as well as on a current state of art system, the advantage in terms of emissions performance improvement (specifically NO_x conversion) was demonstrated. The demonstration was done on an engine dynamometer considering transient cycles well known in the industry.



The Danish Environmental
Protection Agency
Tolderlundsvej 5
DK - 5000 Odense C

www.mst.dk